AD NUMBER

AD813478

LIMITATION CHANGES

TO:

Approved for public release; distribution is unlimited.

FROM:

Distribution authorized to U.S. Gov't. agencies and their contractors; Critical Technology; 15 FEB 1967. Other requests shall be referred to Office of Naval Research, Attn: Code 418, One Liberty Center, 875 North Randolph Street, Arlington, VA 22203-1995. This document contains export-controlled technical data.

AUTHORITY

ONR ltr dtd 2 Mar 1979

ASTROPHYSICS RESEARCH CORPORATION
10889 WILSHIRE BOULEVARD / LOS ANGELES, CALIFORNIA 90024 / (213) 477-2033

RADAR CROSS SECTIONS OF INHOMOGENEOUS PLASMA SPHERES (U)
PART II - APPLICATIONS

TR-018

15 FEBRUARY 1967

SPONSORED BY

OFFICE OF NAVAL RESEARCH
CODE 418
WASHINGTON 25, D.C.
CONTRACT NONR 4527 (00)

ASTROPHYSICS RESEARCH CORPORATION
10889 Wilshire Boulevard
Los Angeles, California 90024

RADAR CROSS SECTIONS OF INHOMOGENEOUS PLASMA SPHERES (U)

PART II - APPLICATIONS

By

Victorr A. Erma

TR-018

15 February 1967

Sponsored by

Office of Naval Research
Code 418
Washington 25, D.C.
Contract Nonr 4527(00)

ABSTRACT

The present work has been concerned with the numerical evaluation of the exact analytical expressions obtained in Part I[1] for the scattering from radially inhomogeneous plasma spheres of different electron density profiles. Several computer programs were developed for this purpose. These programs are capable of handling a wide range of values of the physical parameters, and are of potential value to many research programs concerned with the scattering of electromagnetic waves from plasma spheres. Numerical data were calculated for a number of representative cases characteristic of high-altitude plasma clouds. Configurations of both radially increasing and decreasing electron density profiles were evaluated. The plasma spheres considered generally had radii of 100-200 m, with electron densities of the order $10^{18} m^{-3}$. Radar cross sections for these spheres were computed for the entire range of frequencies. For purposes of greater physical understanding of the numerical results obtained, analytical approximations to the exact expressions were developed for the Rayleigh region. Finally, the existence of the anomalous back-scatter region in the cross section profile of overdense plasmas was confirmed.

TABLE OF CONTENTS

I. INTRODUCTION

The ultimate aim of our overall research program on the radar cross sections of inhomogeneous spherical plasma clouds is to provide a theoretical understanding of all aspects of the radar signatures of such clouds. As a first step in this direction, our initial efforts have been devoted primarily to the question whether ground-based radar cross section measurements can be considered a practicable and useful diagnostic tool for determining the electron density profiles of plasma clouds. We are thus in effect dealing with the so-called "inverse scattering problem", i.e., with the question whether the precise electron density distribution can be unambiguously inferred from the measured radar cross section profile as a function of frequency. As is well-known, the inverse scattering problem is of formidable complexity. Although some limited progress has been achieved for the case of scalar scattering, no significant progress whatever has been reported for the much more complex case of vector scattering with which we are concerned. In fact, not even the problem of uniqueness, i.e., the question whether two plasma spheres of different radii and/or different electron distributions must necessarily give rise to different radar cross section profiles, has been resolved to date.

As indicated above, the inverse scattering problem for vector waves is not amenable to a direct approach. Accordingly, in our present investigation we have chosen to follow an indirect approach; i.e., instead

of attempting to infer the electron distribution of a plasma from a given radar cross section profile, we have calculated the radar cross section profiles of several specified characteristic electron distributions, in the hope that some meaningful correlations may be observed between these two quantities.

It is clear that, apart from possibly the very grossest of features, different characteristic electron distributions will reveal themselves primarily in the so-called "resonance region" of the radar spectrum. Unfortunately, this circumstance complicates the analytical problem considerably, in that it precludes the use of various well-known approximate techniques and necessitates exact solutions of the scattering problem. Toward this end, we have obtained exact analytical solutions for the radar cross sections of various spherically symmetric plasma spheres.[1] These include: The homogeneous sphere; the "spherical shell", consisting generally of a central core and an annular region of differing (complex) refractive indices; a plasma whose refractive index decreases according to the law $n = A/r$; and a plasma whose refractive index increases according to $n = Ar^m$. For all of these cases we were able to obtain analytical solutions for all the scattering quantities of interest. These were reported in Part I of the present research effort.[1]

The present report is concerned with the numerical evaluation of these analytical expressions. This required the development of several very complex computer programs. The fundamental reason for the complexity of these programs and the difficulties encountered in developing

them is that the particular cases of the most interest to us, i.e., high-altitude plasma clouds, involve ranges of the relevant physical parameters which are particularly inconvenient from a mathematical point of view, particularly in the resonance range. Nevertheless, we were successful in developing computer programs capable of handling all cases of interest. These were applied to the numerical calculation of radar cross sections for a number of typical test cases. The particular representative cases computed to date were designed primarily for the purpose of testing the validity of the computer programs over a wide range of frequency rather than to provide a basis for a systematic analysis of the diagnostic value of radar cross section profiles. Considerably more data, corresponding to much wider ranges of the physical parameters, must be obtained before meaningful conclusions concerning the diagnostic possibilities of ground-based radar can be drawn.

Section II of the present report is devoted to deriving approximations to the exact analytical expressions, which are valid in the Rayleigh region ($ka \ll 1$). Although our primary interest lies in the resonance region, because of their analytical simplicity such approximations are useful for the physical interpretation of the exact cross section data. In Section III we describe the particular test cases for which exact numerical computations of the cross sections were carried out, and discuss their physical significance. The methods of numerical evaluation, together with some of their attendant difficulties, are discussed briefly in Section IV. The actual numerical results obtained are contained in Section V. Finally,

Section VI is devoted to such tentative conclusions as may be drawn from the preliminary data obtained so far, as well as indications of future work.

II. APPROXIMATE EXPRESSIONS

Although we have obtained exact numerical results for all cases, it nevertheless remains of interest to consider approximate expressions in regions where such may be obtained. Inasmuch as such approximate expressions generally exhibit the explicit analytical dependence of the scattering quantities on the physical parameters, they are capable of yielding additional physical insight, and are thus useful for the physical interpretation of the exact numerical data.

For our present purposes, our approach to obtaining such approximate expressions will consist of finding the suitable mathematical approximations to the exact analytical solutions obtained earlier in Part I. (The alternate approach would be to find a suitable approximate method to solve the physical problem from the very beginning).

The two regions where the exact mathematical expressions may be simplified are those where the value of $y = ka$ is either very small or very large. Of these two, only the former, corresponding to the so-called Rayleigh region, yields useful results for the cases of interest to us.

Accordingly, we shall first consider the case when $y = ka \ll 1$. In what follows, the notation will be the same as that of Part I. For very small values of the argument, the leading terms of the relevant Bessel functions are well known and are given by

$$J_\nu(\rho) \sim \frac{\rho^\nu}{2^\nu \Gamma(\nu+1)} \tag{1}$$

$$H^{(1)}_{\ell+1/2}(\rho) \sim \frac{-i(-1)^\ell \rho^{-(\ell+1/2)}}{2^{-(\ell+1/2)}\Gamma(-\ell+1/2)} \tag{2}$$

where $\Gamma(x)$ denotes the gamma function. From these, we easily obtain the following first-order expressions:

$$\left.\begin{aligned} \Psi_\ell(\rho) &= \frac{2^\ell \ell!\, \rho^{\ell+1}}{(2\ell+1)!} \\ \zeta^{(1)}_\ell(\rho) &= \frac{-i(2\ell-1)!}{2^{(\ell-1)}(\ell-1)!}\,\rho^{-\ell} \\ \chi_\ell(\rho) &= \frac{-(2\ell-1)!!}{\rho^\ell} \end{aligned}\right\} \tag{3}$$

where $(2\ell-1)!! = (2\ell-1)(2\ell-3)\cdots 3.1$.

From these in turn we may calculate:

$$\left.\begin{aligned} D_\ell(\rho) &= \frac{(\ell+1)}{\rho} \\ \Gamma_\ell(\rho) &= \frac{-\ell}{\rho} \\ E_\ell(\rho) &= \frac{\ell}{\rho} \end{aligned}\right\} \tag{4}$$

The following relationships, which may be obtained from the above results, will be found to be useful:

$$\left.\begin{aligned} \zeta_\ell^{(1)}(\rho) &= \frac{1}{i\Psi_{\ell-1}(\rho)} \\ \Gamma_\ell(\rho) &= -D_{\ell-1}(\rho) \\ \Gamma_\ell(\rho) &= -E_\ell(\rho) \end{aligned}\right\} \qquad (5)$$

We shall now use the above approximations in order to simplify the expression for the radar cross section for the case of a spherical shell. (Interior radius $a, y = ka$, interior refractive index n_3; outer radius $b, x = kb$, annular refractive index n_2.) The scattering coefficients for this case are given by expressions (53) and (54) of the next section.

To begin with, we note that in order to obtain a first order result for the cross section, we need to retain only the first-order coefficients ${}^{e}B_1$ and ${}^{m}B_1$. Thus, the infinite series for the cross section reduces to a single term. If we desired to improve the result by including the second-order coefficients ${}^{e}B_2$ and ${}^{m}B_2$, we would for the sake of consistency also have to include higher-order terms in the Bessel functions entering into ${}^{e}B_1$ and ${}^{m}B_1$ (i.e., the approximations (1) - (5) would be inadequate for calculating ${}^{e}B_1$ and ${}^{m}B_1$).

Thus, restricting our attention to the first-order results, the various quantities entering into expressions (53) and (54) are found to be given by

$$\Psi_1(x) = \frac{x^2}{3} \quad , \quad \Psi_1(n_2 x) = \frac{n_2^2 x^2}{3} \quad , \quad \Psi_1(n_2 y) = \frac{n_2^2 y^2}{3}$$

$$\zeta_1^{(1)}(x) = \frac{-i}{x}$$

$$\left.\begin{aligned} \chi_1(n_2 y) = -\frac{1}{n_2 y} \quad , \quad \chi_1(n_2 x) = -\frac{1}{n_2 x} \\ D_1(x) = \frac{2}{x} \quad , \quad D_1(y) = \frac{2}{y} \quad , \quad D_1(n_2 x) = \frac{2}{n_2 x} \quad , \quad D_1(n_3 y) = \frac{2}{n_3 y} \\ E_1(n_2 y) = \frac{1}{n_2 y} \quad , \quad E_1(n_2 x) = \frac{1}{n_2 x} \\ \Gamma_1(x) = -\frac{1}{x} \end{aligned}\right\} \quad (6)$$

where we have assumed that y and x are sufficiently small such that all arguments occurring above are small in absolute magnitude.

Substituting these expressions into Eq. (53) for ${}^{e}B_1$, we obtain

$${}^{e}B_1 = -\frac{ix^3}{3}\left(\frac{A}{B}\right) \quad (7)$$

where

$$A = \frac{-n_2 x^2}{3y}\left[\frac{2n_2}{x} - \frac{2}{n_2 x}\right]\left[\frac{2n_2}{n_3 y} - \frac{n_3}{n_2 y}\right] + \frac{n_2 y^2}{3x}\left[\frac{2n_2}{x} - \frac{1}{n_2 x}\right]\left[\frac{2n_2}{n_3 y} - \frac{2n_3}{n_2 y}\right] \quad (8)$$

$$B = \frac{n_2 x^2}{3y}\left[\frac{n_2}{x} + \frac{2}{n_2 x}\right]\left[\frac{2n_2}{n_3 y} - \frac{n_3}{n_2 y}\right] - \frac{n_2 y^2}{3x}\left[\frac{n_2}{x} - \frac{1}{n_2 x}\right]\left[\frac{2n_2}{n_3 y} - \frac{2n_3}{n_2 y}\right] \quad (9)$$

We shall now consider the special case $x = 2y$ (corresponding to the examples listed under Case II of Section III below). After substituting $x = 2y$, and simplifying, we finally obtain the following first-order expression for ${}^{e}B_1$:

$$ {}^{e}B_1 = \frac{16}{3} iy^3 \frac{\left[\left(n_2^2 - 1\right)\left(2n_2^2 - n_3^2\right) - \frac{1}{8}\left(2n_2^2 - 1\right)\left(n_2^2 - n_3^2\right)\right]}{\left[\left(n_2^2 + 2\right)\left(2n_2^2 - n_3^2\right) - \frac{1}{4}\left(n_2^2 + 1\right)\left(n_2^2 - n_3^2\right)\right]} $$

We now turn to the corresponding expression for ${}^{m}B_1$, given by Eq. (54). It is easily seen that the first-order expression for ${}^{m}B_1$ vanishes, inasmuch as

$$ \left[D_1(x) - n_2 D_1(n_2 x)\right] = 0 \quad , \quad \left[n_3 D_\ell(n_3 y) - n_2 D_\ell(n_2 y)\right] = 0 $$

to first order. Accordingly, in order to obtain the first non-vanishing term of ${}^{m}B_1$, we must consider the next order term in our approximation for D_ℓ. This may be obtained from the second term in the power series expansion of the Bessel function, and we find

$$ D_1(\rho) \sim \frac{2}{\rho} - \frac{\rho}{5} \tag{11} $$

Substituting this approximation into (54), we find after some computation

$$ {}^{m}B_1 = -\frac{ix^3}{3}\left(\frac{C}{D}\right) \tag{12} $$

where

$$C = -\frac{n_2 x^2}{3y}\left[\frac{2}{x} - \frac{x}{5} - n_2\left(\frac{2}{n_2 x} - \frac{n_2 x}{5}\right)\right]\frac{1}{y} + \frac{n_2 y^2}{3x}\left[n_3\left(\frac{2}{n_3 y} - \frac{n_3 y}{5}\right) - n_2\left(\frac{2}{n_2 y} - \frac{n_2 y}{5}\right)\right]\frac{1}{x} \tag{13}$$

$$D = \frac{n_2 x^2}{3y}\left(\frac{3}{x}\right)\left(\frac{1}{y}\right) - \frac{n_2 y^2}{3x}\left(\frac{2}{x}\right)\left[n_3\left(\frac{2}{n_3 y} - \frac{n_3 y}{5}\right) - n_2\left(\frac{2}{n_2 y} - \frac{n_2 y}{5}\right)\right] \tag{14}$$

If we now again consider the case $x = 2y$, and keep only consistent orders, we finally obtain the following expression for the first non-vanishing term of ${}^{m}B_1$:

$${}^{m}B_1 = -\frac{32}{45} i y^5 \left[\left(n_2^2 - 1\right) + \frac{1}{32}\left(n_2^2 - n_3^2\right)\right] \tag{15}$$

We note that this is of higher order in y than the corresponding expression for the first non-vanishing term of ${}^{e}B_1$.

We now turn briefly to the other extreme where $y = ka >> 1$. For the range of physical parameters of most practical interest, the arguments of the Bessel functions will generally be very large compared to their order. Although approximate asymptotic expressions for the Bessel functions are well known for this case, they do not lead to a useful approximation to the radar cross section. The reason for this is that we must keep a very large

number of terms in the infinite series for the cross section; accordingly, we do not obtain any single or easily surveyable analytic expression in this region, which might aid us in interpreting the data physically. On the other hand, this region corresponds to the so-called region of geometrical optics, whose principles may be applied in this case. Thus, for instance, we may recall the familiar result that the radar cross section of non-absorbing plasma spheres approaches the geometrical cross section for $ka \gg 1$. Accordingly, beyond the overall radius of the plasma sphere, the radar cross section in this region provides no information about the magnitude or spatial distribution of the electron density.

III. DESCRIPTION OF CASES CONSIDERED

A. GENERAL

Exact numerical values for the radar cross section profiles of plasma spheres as a function of frequency have been computed for several typical test cases, corresponding to the various refractive index functions for which analytical solutions were obtained in Part I of this work. These include the following major configurations:

1. Homogeneous sphere; $r = a$,

   refractive index $n(r) = \text{const.}$

2. Spherical Shell;

$$n(r) = \begin{cases} n_3 = \text{const.}, & o<r<a \\ n_2 = \text{const.}, & a<r<b \end{cases}$$

3. Decreasing Refractive Index;

$$n(r) = \begin{cases} n_3 = \text{const.}, & o<r<a \\ A/r, & a<r<b \end{cases}$$

4. Increasing Refractive Index;

$$n(r) = \begin{cases} n_3 = \text{const.}, & o<r<a \\ Br, & r<b \end{cases}$$

Wherever possible, both real and complex values for $n(r)$ were considered. (The latter corresponds to the presence of absorption.)

In all cases, the refractive index n is related to the physical parameters describing the plasma by means of the well-known expression

$$\epsilon = 1 - \frac{n_e e^2 (1 - i\nu_c/\omega)}{m\epsilon_o(\omega^2 + \nu_c^2)} \tag{15}$$

$$n = \epsilon^{1/2} \tag{16}$$

Here n_e is the electron density, e is the electronic charge, m the electronic mass, ϵ_o is the permittivity of the vacuum, ν_c is the collision frequency, and ω is the angular frequency of the incident wave. We should also note that Eq. (15) employs MKS units throughout, and that the sign of the square root in Eq. (16) should be taken such that $\mathrm{Im}(n)>o$. Finally, the electron density n_e is generally a function of position r.

It is converient to rewrite Eqs. (15) and (16) in terms of the dimensionless parameter $y = ka$ ($k = 2\pi/\lambda$, where λ is the wavelength of the incident wave). Thus, noting that $\omega = kc$, Eq. (15) can be rewritten in the form

$$\epsilon = 1 - \frac{\gamma}{(y^2+\delta^2)}\left(1 - i\frac{\delta}{y}\right) = 1 - \frac{\gamma}{y(y+i\,\delta)} \tag{17}$$

where we have introduced the dimensionless parameters

$$\gamma = \frac{n_e e^2 a^2}{m\epsilon_o c^2}, \quad \delta = \frac{\nu_c a}{c} \tag{18}$$

Accordingly, Eq. (16) becomes

$$n = \left[1 - \frac{\gamma}{y(y+i\delta)} \right]^{1/2} \tag{19}$$

We note that for constant a, γ is directly proportional to the electron density n_e. Furthermore, in the frequently occurring case when $\frac{\gamma}{y(y+i\delta)} >> 1$, we obtain the approximate proportionality

$$n \propto \sqrt{n_e} \tag{20}$$

Finally, the total number of electrons contained within the plasma sphere is given by

$$N = 4\pi \int_0^R n_e(r) r^2 dr$$

where R is the outer radius of the plasma sphere.

At this time we should take note of the following important point. The quantity which enters directly into the original differential equations is not the electron density n_e, but the refractive index n. As we have seen in Part I, analytic solutions of these differential equations can be obtained only for a few specific variations of n(r) as a function of r. These particular functions n(r) may or may not correspond to physically meaningful electron densities. Whether or not they do depends both on the particular function, as well as on the relative magnitudes of the physical parameters involved. (Thus, for

certain functions n(r) and certain ranges of the physical parameters, the corresponding electron densities would be complex or frequency-dependent, neither of which represents a physically meaningful situation). This question must be investigated individually for each of the cases considered.

In what follows, we list the relevant parameters for all of the cases for which radar cross sections have been computed to date. We should like to emphasize that the calculations performed to date do not constitute a systematic or exhaustive study which spans the entire range of the physical parameters of interest. They merely represent certain representative cases, designed primarily to demonstrate the versatility of the numerical program. The physical parameters chosen for these test cases involve sphere radii of the order of 100 - 200 m, electron densities of the order of $10^{18}/m^3$, and collision frequencies of the order of 10^{10}/sec. The frequency was varied over the entire range of interest.

B. CASE I - HOMOGENEOUS SPHERE

Several sub-cases were considered. These are described by the following parameters:

Subcase (a)

$$\left.\begin{array}{l} n_e = 10^{18}/m^3 \; ; \; a = 100 \text{ m} \; , \; \nu_c = 0 \\ n \text{ defined by } \quad \gamma = 3.54164 \times 10^8 \; , \; \delta = 0 \\ N = 4.189 \times 10^{24} \end{array}\right\} \qquad (22)$$

Subcase (b)

$$\left.\begin{array}{l} n_e = 10^{18}/m^3 \; ; \; a = 100 \text{ m}, \; \nu_c = 10^{10}/\text{sec} \\ \text{n defined by: } \gamma = 3.54164 \times 10^{8}, \; \delta = 3.33564 \times 10^{3} \\ N = 4.189 \times 10^{24} \end{array}\right\} \quad (23)$$

Subcase (c)

$$\left.\begin{array}{l} n_e = 1.25 \times 10^{17}/m^3 \; ; \; a = 200 \text{ m}, \; \nu_c = 0 \\ \text{n defined by: } \gamma = 4.42705 \times 10^{7} \; , \; \delta = 0 \\ N = 4.189 \times 10^{24} \end{array}\right\} \quad (24)$$

The electron density profiles of the above three cases are shown in Figures 1 and 2.

All three of the above cases represent plasma spheres with an equal total number of electrons, Cases I(a) and I(b) are identical except for the fact that Case I(b) represents an absorbing sphere, while I(a) is a non-absorbing sphere. Similarly, Case I(c) differs from I(a) in that the same total number of electrons is spread out over a sphere of twice the radius.

In addition, we also considered the special case:

Subcase (d)

$$\left.\begin{array}{l} a = 1.5 \text{ m} \; , \; \nu = 2\pi\nu = 1.27236 \times 10^{9}/\text{sec} \\ \nu_c = 10^{10}/\text{sec} \qquad (ka = 40) \end{array}\right\} \quad (25)$$

In this case the variable parameter is the electron density (and hence γ).

C. CASE II - SPHERICAL SHELL

For all of the spherical shell cases considered, we have chosen

$$\frac{x}{y} = \frac{b}{a} = 2 \text{ ; with } a = 100 \text{ m , } b = 200 \text{ m}$$

The various cases differ in their interior and annular electron densities, as well as generally in the total number of electrons. If n_{e_3} and n_{e_2} represent the interior and annular electron densities, respectively, the total number of electrons is given by

$$N = \frac{4}{3}\pi a^3 (n_{e_3} + 7 n_{e_2}) \tag{26}$$

In order to describe the subcases considered most compactly, we define a particular reference refractive index n_1 by means of:

$$n_1 \text{ defined by } \gamma_1 = 3.54164 \times 10^8, \ \delta_1 = 3.33564 \times 10^3 \tag{27}$$

This corresponds to the physical parameters of Case I(b). If n_3 and n_2 denote the interior and annular refractive indices, respectively, the various subcases considered are then as follows:

Subcase (a)

$$n_3 = n_1 \; ; \; n_2 = \frac{n_1}{3} \; ; \quad N = 7.45 \times 10^{24} \tag{28}$$

Subcase (b)

$$n_3 = \frac{n_1}{3} \; ; \; n_2 = n_1 \; ; \; N = 2.98 \times 10^{25} \tag{29}$$

Note that Case II(b) differs from Case II(a) in that the interior and annular refractive indices have been interchanged.

Subcase (c)

$$n_3 = 2.64575\, n_1 \; , \; n_2 = 0.125988\, n_1 \; ; \; N = 2.98 \times 10^{25} \tag{30}$$

Subcase (c) was designed to have the same total number of electrons as II(b); however, all of the electrons which were in the interior region of II(b) are in the annular region of II(c), and vice versa.

Subcase (d)

$$n_3 = 0.881917\, n_1 \; , \; n_2 = 0.3779645\, n_1 \; ; \; N = 7.45 \times 10^{24} \tag{31}$$

Case II(d) bears the same physical relation to II(a) as Case II(c) bears to II(b).

Subcase (e)

Let n_1' be defined by: $\gamma_1' = 3.54164 \times 10^{8}$, $b_1' = 0$ (32)

Subcase (e) is then defined by:

$$n_3 = 0.5477226\, n_1' \,,\; n_2 = 0.3162278\, n_1' \,;\quad N = 4.189 \times 10^{24} \tag{33}$$

This represents a spherical shell case which has the same total of electrons as Case I(a). In addition, the interior electron density is three times the annular electron density. Moreover, there is no absorption, so that this case is most directly comparable with Case I(a), from which it differs only in the electron distribution.

Subcase (f)

$$n_3 = 0.2132007\, n_1' \,,\; n_2 = 0.369274\, n_1' \,;\; N = 4.189 \times 10^{24} \tag{34}$$

where n_1' is again given by (32). This case is similar to Case II(e), except that here the annular electron density is three times the interior density.

The actual electron density profiles for Cases II(a) - (b) are illustrated in Figures 3 - 8.

D. CASE III - DECREASING REFRACTIVE INDEX

Here we consider the case where the refractive index is given by

$$n(r) = \begin{cases} n_3 \,, & 0<r<a \\ \dfrac{A}{kr} \,, & a<r<b \end{cases} \tag{35}$$

i.e., in effect a spherical shell whose interior region has a uniform refractive index, while the refractive index of the annular region decreases.

For the sake of continuity at r = a, we must take

$$A = n_3 y \ , \ (y = ka) \tag{36}$$

To begin with, we must investigate whether the above function corresponds to a physically meaningful electron density. We recall that γ is proportional to the electron density. From Eq. (19), together with (35) and (36), we then obtain

$$\left(\frac{n_3 a}{r}\right)^2 = 1 - \frac{\gamma}{y(y+i\delta)} \tag{37}$$

On the other hand n_3^2 itself is generally defined by

$$n_3^2 = 1 - \frac{\gamma_3}{y(y+i\delta_3)} \tag{38}$$

Substituting (38) into (37), we obtain

$$\frac{a^2}{r^2}\left(1 - \frac{\gamma_3}{y(y+i\delta_3)}\right) = 1 - \frac{\gamma}{y(y+i\delta)} \tag{39}$$

From (39) we can immediately see that we will not obtain a real value for γ (or n_e) for any relative magnitude of the physical parameters, unless $\delta_3 = \delta = o$. Thus, Eq. (35) corresponds to a real electron

density only for the case of no absorption. With this, Eq. (39) becomes

$$\frac{a^2}{r^2}\left(1 - \frac{\gamma_3}{y^2}\right) = 1 - \frac{\gamma}{y^2} \tag{40}$$

We are still faced with the problem that γ will in general depend on the frequency ($y = ka$), which is again not physically meaningful for our problem. However, we note that if both

$$\frac{\gamma_3}{y^2} \gg 1 \quad \text{and} \quad \frac{\gamma}{y^2} \gg 1 \tag{41}$$

i.e., the plasmas are effectively "overdense", then Eq. (40) reduces to the physically meaningful equation

$$\gamma = \frac{\gamma_3 a^2}{r^2} \tag{42}$$

which is equivalent to

$$n_e = \frac{n_{e_3} a^2}{r^2} \tag{42'}$$

as long as both γ and γ_3 were calculated with the same value of $\underline{a}$ (Cf. Eq. (18)). In the cases of interest to us, both γ and γ_3 are of the order of magnitude 10^8 while y ranges from 0 to 100. Accordingly, the conditions (41) are well satisfied, and the results obtained correspond to a physically meaningful electron density.

As can be seen from Eq. (42), the electron density n_e in the annular region decreases as r^{-2}, corresponding to the refractive index (35).

Finally, it is a simple matter to show that for this case the total number of electrons is given by

$$N = \frac{4}{3}\pi a^3 n_{e_3}\left[1 + 3\left(\frac{b}{a} - 1\right)\right] \tag{43}$$

As typical test cases for purposes of comparison, we have calculated two subcases:

Subcase (a)

$$\left.\begin{array}{c} \frac{b}{a} = 2\ ;\ a = 100\,\text{m}\ ,\ b = 200\,\text{m} \\ n_3 \text{ defined by: } \gamma_3 = 3.54164 \times 10^{8}\ ,\ \delta_3 = 0 \\ N = 1.68 \times 10^{25} \end{array}\right\} \tag{44}$$

Subcase (b)

$$\left.\begin{array}{c} \frac{b}{a} = 20\ ;\ a = 10\,\text{m}\ ,\ b = 200\,\text{m} \\ n_3 \text{ defined by: } \gamma_3 = 6.106276 \times 10^{7}\ ,\ \delta_3 = 0 \\ N = 4.189 \times 10^{24} \end{array}\right\} \tag{45}$$

This subcase corresponds to the same total number of electrons as Case I(a), and several of the subcases of Case II.

The actual electron density profiles of Cases II(a), (b) are shown in Figures 9 - 10.

E. CASE IV - INCREASING REFRACTIVE INDEX

This case corresponds to a refractive index given by

$$n(r) = \begin{cases} n_3 , & 0<r<a \\ B(kr) , & a<r<b \end{cases} \tag{46}$$

Again we take $B = n_3/y$ for continuity. Here we have a homogeneous central core, and an annular region in which the refractive index is increasing.

As in the preceding case, we must investigate the question whether the above refractive index leads to a physically meaningful electron density. The analysis is similar to that carried out for Case II. Without going into detail, we find that we do indeed obtain a physically meaningful density, provided that $\delta = \delta_3 = o$ and $\gamma_3/y^2 >> 1$. Both of these conditions are fulfilled for all cases of interest to us. The electron density in the annular region as a function of radius is given by

$$n_e = n_{e_3} \left(\frac{r}{a}\right)^2 \tag{47}$$

where n_{e_3} is the electron density in the interior core. Similarly, the total number of electrons is

$$N = \frac{4}{3}\pi n_{e_3} a^3 \left[1 + \frac{3}{5}\left(\frac{b^5}{a^5} - 1\right)\right] \tag{48}$$

The following subcases were computed:

Subcases (a)

$$\left.\begin{array}{c} b/a = 2 \; ; \; a = 100\,m \; , \; b = 200\,m \\ n_3 \text{ defined by: } \gamma_3 = 3.54164 \times 10^8 \; , \; \delta_3 = 0 \\ N = 8.22 \times 10^{25} \end{array}\right\} \tag{49}$$

This case corresponds to the interior density being the same as that of the homogeneous sphere I(a).

Subcase (b)

$$\left.\begin{array}{c} b/a = 2 \; ; \; a = 100\,m \; , \; b = 200\,m \\ n_3 \text{ defined by: } \gamma_3 = 8.8541 \times 10^7 \; , \; \delta_3 = 0 \\ N = 2.055 \times 10^{25} \end{array}\right\} \tag{50}$$

In this case the electron density at the outer edge (r = b) is the same as that of the homogeneous sphere I(a).

Subcase (c)

$$\left.\begin{array}{c} b/a = 20 \; ; \; a = 10\,m \; , \; b = 200\,m \\ n_3 \text{ defined by: } \gamma_3 = 7.227836 \times 10^{7} \; , \; \delta_3 = 0 \\ N = 1.64 \times 10^{29} \end{array}\right\} \quad (51)$$

Subcase (d)

$$\left.\begin{array}{c} b/a = 20 \; ; \; a = 10\,m \; , \; b = 200\,m \\ n_3 \text{ defined by: } \gamma_3 = 1.844604 \times 10^{3} \; , \; \delta_3 = 0 \\ N = 4.189 \times 10^{24} \end{array}\right\} \quad (52)$$

This case corresponds to the same total number of electrons as Case I(a) and several other cases considered above.

The actual electron density profiles corresponding to the above subcases of Case IV are illustrated in Figures 11 - 14.

IV. METHODS OF CALCULATION

In Part I of the present work we developed exact analytical expressions for the scattering coefficients ${}^{e}B_{1}$ and ${}^{m}B_{1}$ for all of the cases detailed in the preceding section. Thus, the expressions for ${}^{e}B_{1}$ and ${}^{m}B_{1}$ for Case I are given by Eqs. I-123 and I-124. (Equation I-x means Eq. (x) of Part I). The corresponding expressions for Cases III and IV are given by Eqs. I-197, 198 and Eqs. I-155, 156 (together with I-206-211), respectively. The spherical shells considered in Part I had an interior core whose refractive index was unity. Thus, expressions I-172, 173 for ${}^{e}B_{1}$ and ${}^{m}B_{1}$, developed in Part I, are not sufficiently general for the examples of Case II considered here, for which the interior index differs from unity. However, Eqs. I-172, 173 are easily generalized; the result is:

$$e_{B_\ell} = \left(-\frac{\psi_\ell(x)}{\zeta_\ell^{(1)}(x)}\right)\left\{\frac{\psi_\ell(n_2x)\chi_\ell(n_2y)[n_2D_\ell(x)-D_\ell(n_2x)][n_2D_\ell(n_3y)-n_3E_\ell(n_2y)]-\psi_\ell(n_2y)\chi_\ell(n_2x)[n_2D_\ell(x)}{\psi_\ell(n_2x)\chi_\ell(n_2y)[n_2\Gamma_\ell(x)-D_\ell(n_2x)][n_2D_\ell(n_3y)-n_3E_\ell(n_2y)]-\psi_\ell(n_2y)\chi_\ell(n_2x)[n_2\Gamma_\ell(x)}\right.$$

$$\left.-\frac{E_\ell(n_2x)][n_2D_\ell(n_3y)-n_3D_\ell(n_2y)]}{E_\ell(n_2x)][n_2D_\ell(n_3y)-n_3D_\ell(n_2y)]}\right\} \tag{53}$$

$$m_{B_\ell} = \left(-\frac{\psi_\ell(x)}{\zeta_\ell^{(1)}(x)}\right)\left\{\frac{\psi_\ell(n_2x)\chi_\ell(n_2y)[D_\ell(x)-n_2D_\ell(n_2x)][n_3D_\ell(n_3y)-n_2E_\ell(n_2y)]-\chi_\ell(n_2x)\psi_\ell(n_2y)[D_\ell(x)}{\psi_\ell(n_2x)\chi_\ell(n_2y)[\Gamma_\ell(x)-n_2D_\ell(n_2x)][n_3D_\ell(n_3y)-n_2E_\ell(n_2y)]-\chi_\ell(n_2x)\psi_\ell(n_2y)[\Gamma_\ell(x)}\right.$$

$$\left.-\frac{n_2E_\ell(n_2x)][n_3D_\ell(n_3y)-n_2D_\ell(n_2y)]}{n_2E_\ell(n_2x)][n_3D_\ell(n_3y)-n_2D_\ell(n_2y)]}\right\} \tag{54}$$

where the refractive index is defined by

$$n(r) = \begin{cases} n_3\,, & 0 < r < a \\ n_2\,, & a < r < b\,, \end{cases} \tag{55}$$

and the remainder of the notation is as in Part I.

All of the cases listed in the preceding section were programmed for numerical evaluation on an IBM-7094 Computer. Unfortunately, this turned out to be a far from trivial task; a number of fundamental and unexpectedly very time-consuming difficulties were encountered. To begin with, the exact expressions are exceedingly cumbersome and involve the rather complicated Ricatti-Bessel functions. Secondly, the particular cases of interest to us, corresponding to high-altitude plasma clouds, involve a range of the relevant physical parameters which is especially inconvenient to handle numerically. Furthermore, the expressions become mathematically "pathological" in the resonance region, which is the region of the greatest significance for our purpose. This latter fact is of course not accidental. Inasmuch as the resonance region by virtue of its very nature involves large oscillations in the values of the cross section, it is only to be expected that in this region the mathematical functions do not behave "smoothly", but change rapidly even for small changes in the wavelength.

It was originally contemplated that all of the four cases to be treated would be handled by a single program. To begin with, this required writing a new Bessel function subroutine more general than those existing in program libraries, such as SHARE. The wide range in the orders and arguments of the Bessel functions alone required that the Bessel function subroutine treat four distinct cases. This necessitated some sort of uniform scaling, inasmuch as for arguments with large imaginary parts the magnitude of the Bessel function exceeded the range of the computer registers. Secondly,

the program, when written, was too large to be loaded into the machine memory. Accordingly, it was decided to treat each of the four cases by a separate program.

Cases I, II, III required only Bessel functions of half-integral order; these could be generated by means of simple recursion techniques. Apart from minor difficulties, Cases I and III presented no additional special problems.

The case of the spherical shell (Case II) required further analysis, however. For the particular range of parameters considered, the analytical expressions for ${}^{e}B_{1}$ and ${}^{m}B_{1}$ became indeterminate (0/0) to within the accuracy of the computer. This problem arose whenever the index of refraction had a large imaginary part (Im $(n_3 y) > 10$, for example). It was first thought that multiple precision arithmetic could be used to circumvent this difficulty, but a trial calculation showed that even this would be inadequate. The problem was finally overcome by expressing the Ricatti Bessel functions in terms of sines and cosines, which made it possible to analytically subtract the large parts in differences such as $\psi_\ell(z_1)\chi_m(z_2) - \psi_m(z_2)\chi_\ell(z_1)$. The remainder could then be generated by appropriate recursion methods. Even with this approach, the range of values of the functions generated approaches the limits of the capacity of the IBM-7094 Computer.

Case IV likewise required special attention. Here we must evaluate Bessel functions of generally non-rational order, for very large complex values of the argument. A general Bessel function routine, using an extra

location in storage, was written to calculate these values. This subroutine worked well, but required excessive computation time. After considerable further modification, the computation time could be reduced to a reasonable level.

After considerable effort, all of the aforementioned difficulties were finally surmounted, and successful programs were obtained for all four cases considered. Wherever possible, the results obtained were checked either by laborious hand calculation or by comparison with known results. The successful development of computer programs capable of handling all four cases, at least for the range of physical parameters hitherto considered, represents one of the primary accomplishments of this stage of our general research program.

V. NUMERICAL RESULTS FOR CROSS SECTIONS

Numerical results for the radar - (and in most cases extinction -) cross sections as a function of frequency have been obtained for all of the cases described in Section III. The values of $y = ka$ for which the cross sections were calculated ranged from $y = 0$ to $y = 140$, although for reasons of simplicity the curves presented extend only up to values of y at which the cross sections attain their asymptotic values. The results obtained are presented in the present section. Inasmuch as the particular cases considered represent only representative test cases characteristic of the range of physical parameters of the greatest interest, rather than any effort toward a comprehensive analysis, we shall for the most part simply present the results without detailed discussion or interpretation.

A. CASE I

The radar cross sections as a function of y for cases I-A and I-C are presented in Figures 15 and 16, respectively. These two cases represent homogeneous spheres containing the same number of electrons; however, the sphere of Case I-C has twice the radius (and hence 1/8 of the electron density) of that of Case I-A. As can be seen from Figures 15 and 16, the normalized radar cross sections are for all practical purposes identical, even in the resonance region. Thus, for homogeneous spheres of the order of magnitude of radius and electron density considered here, the actual measured radar cross section is primarily indicative only of the radius of the

plasma sphere.

In addition to the above cases, we also obtained numerical values for the normalized radar cross section for Case I-D. This differs from the preceding cases in that we are dealing with a small sphere (radius = 1.5 m) and keeping $y = ka$ fixed while varying the electron density. The particular case considered is identical to that calculated by Wyatt[2]. The purpose for considering it here was to ascertain whether our program confirmed the anomalous behaviour found by Wyatt. Indeed, the results obtained were identical to those reported by Wyatt. For the particular values of the radii and electron densities of interest to us, however, this anomalous region corresponds to values of y of the order of $y \sim 10^4$, which are outside the range of our present considerations.

B. CASE II

These cases correspond to spherical shells. It is of particular interest to compare the results for Cases II-A and B, which are presented in Figures 17 and 18, respectively. In Case II-B, the refractive indices of the interior and exterior portions of Case II-A have been interchanged. We may observe that while there do exist differences in the radar cross sections for these two cases, these differences are not very pronounced, and are in fact overshadowed by the similarities. The main difference is that the radar cross section of II-B is somewhat

less than that of II-A (particularly for large y), which can be attributed to the increased absorption present in Case II-B.

In order to try to understand why the results for these two cases should be so similar, despite the fact that the refractive indices (and hence the internal electron density distributions) of the two cases are quite different, it is useful to consider the approximations developed in Section II for the Rayleigh region ($y \ll 1$) . Accordingly, we shall calculate the approximate values of ${}^{e}B_1$ and ${}^{m}B_1$ for both Cases II-A and II-B. To obtain ${}^{e}B_1$ for Case II-A, we thus substitute $n_3 = N$, $n_2 = 3N$ into Eq. (10). This yields:

$$\text{II-A:} \quad {}^{e}B_1 = \frac{16}{3} iy^3 \frac{(135N^2 - 16)}{(135N^2 + 32)} \tag{56}$$

Similarly, for Case II-B, we substitute $n_3 = 3N$, $n_2 = N$ into Eq. (10), which leads to

$$\text{II-B:} \quad {}^{e}B_1 = \frac{16}{3} iy^3 \frac{(5N^2 - 6)}{(5N^2 + 12)} \tag{57}$$

In our case $|N^2| \gg 1$ (particularly for small y); thus, although the analytical forms of (56) and (57) are different, for $|N^2| \gg 1$ they lead to the same value of ${}^{e}B_1$ and hence for the cross section) for both Cases II-A and II-B. Accordingly, the similarity in the cross sections for these two cases can be attributed to the fact that for the particular spheres we are considering the values of N^2 are very large. The corresponding

Rayleigh expressions for ${}^{m}B_1$ for these two cases are found to be

$$\text{II-A:}\quad {}^{m}B_1 = -\frac{32}{45} iy^5 \left(\frac{37}{4} N^2 - 1\right) \tag{58}$$

$$\text{II-B:}\quad {}^{m}B_1 = -\frac{32}{45} iy^5 \left(\frac{3}{4} N^2 - 1\right) \tag{59}$$

Although these expressions do differ, even for $|N^2| \gg 1$, ${}^{m}B_1$ is of higher order in y than ${}^{e}B_1$. Furthermore, in the expression for the cross section this difference may be diminished by the corresponding higher-order terms of ${}^{e}B_1$, which must be kept for consistency.

If we further compare Case II-B with the homogeneous sphere Case I-A, we may observe that the resonance peaks and their locations coincide rather closely for both cases. On the other hand, while the absolute radar cross section values of Case II-B are higher than those of I-A, the normalized cross sections are considerably smaller. Again, this may be attributed to the absorption present in Case II-B.

The results for Cases II-C, D, E, F are presented in Figures 19-22, respectively. Without going into detail, we find that all of these cases are very similar, as far as the location, separation, and magnitude of their resonance peaks is concerned. We should note, however, that this similarity exists only if we consistently plot the cross section as a function of the dimensionless wavelength ratio corresponding to

the outer radius (x = kb in some cases, y = ka in others). While small differences are found to exist in the detailed radar cross section profiles (e.g., between II-C and II-D), these are not of sufficient significance to be of practical diagnostic value.

C. CASE III

The results obtained for Cases III-A and B are presented in Figures 23 and 24, respectively. The cross section profiles of the two cases differ by a factor of 10^2, but are otherwise similar in their behaviour. It is clear that the factor 10^2 arises from the ratio $\left(\frac{x}{y}\right)^2 = \left(\frac{b}{a}\right)^2$, which differs by a factor of 10^2 for the two cases. Comparison with Case I-A shows that the location of the resonance peaks is the same in both cases, although their magnitude differs.

D. CASE IV

The cross sections calculated for Cases IV-A, B, C, D are presented in Figures 25 and 26. Here we find the remarkable result that Cases A and B yield almost identical cross sections; the same is true of Cases C and D. On the other hand, Cases (A, B) differ from (C, D) by a factor of 10^2. This difference is easily accounted for by the difference in the scale factor $\left(\frac{x}{y}\right)^2 = \left(\frac{b}{a}\right)^2$ (Cf. also the discussion of Case III). Thus, the cross section appears to be characteristic of the radius of the interior core rather than the outer radius of the plasma sphere. The results for Case IV are of particular

interest inasmuch as they demonstrate that the inverse scattering problem does not in all cases have a unique solution (at least as far as backscatter cross sections are concerned). Thus, for example, although Cases IV-C and IV-D are physically quite different, they lead to identical radar cross section profiles as a function of frequency.

VI. CONCLUSIONS

During this stage of our overall research program, devoted to the radar signatures of inhomogeneous plasma spheres, we accomplished the following:

(a) Analytical approximations for the exact expressions derived in Part I were developed for the Rayleigh region. These are of value in the physical interpretation of the exact cross section data.

(b) Computer programs for the numerical evaluation of the exact analytical expressions obtained earlier were successfully developed for all cases of interest. Considerable difficulties were encountered, because of the particular ranges of the physical parameters involved in the cases of most practical interest. The development of these computer programs, capable of handling the entire range of the various parameters of interest, represents a major portion of the effort during this stage of our research program.

(c) The cross section profiles as a function of frequency were computed for a number of representative cases, characteristic of high-altitude plasma spheres. The calculations were performed for the entire frequency spectrum, ranging from the Rayleigh region, through the resonance region, to the geometrical optics limit. The plasma spheres considered had radii of 100-200 m, the electron densities in most cases were of the order of $10^{18} m^{-3}$, and a number of different electron density distributions were considered. A total of 15

different cases were computed; these are described in Section III. Both absorbing and non-absorbing plasma spheres were represented. The results obtained represent cross sectional data for plasma spheres of radii and electron density distributions, for which no previous theoretical data have been available.

(d) The existence of the anomalous backscatter region in the cross section profile of overdense plasmas, reported by Wyatt[2], was confirmed.

As a result of our efforts to date, we have succeeded in developing computer programs which enable us to calculate the radar cross sections of plasma spheres for a wide range of the relevant physical parameters. These computer programs are of potential value in a wide variety of research programs concerned with the radar signatures of plasma spheres. The actual examples for which numerical calculations were carried out have been chosen primarily as representative cases which demonstrate the accuracy and versatility of the computer programs developed. The actual numerical data computed to date are as yet insufficient to warrant drawing any meaningful conclusions concerning the question of whether radar cross section measurements can be considered as a useful tool in diagnosing the electromagnetic structure of plasma spheres. Such conclusions must be deferred until a more systematic study, involving considerably more data and a greater variation of the relevant physical parameters, is completed. The present study has provided us with the

calculational means by which such a comprehensive research program may be prosecuted. Future work should be concerned with obtaining considerably more data; in particular, as a function of the other parameters, such as the plasma sphere radius (or ratio of outer to inner radii for shell configurations), electron density, collision frequency, etc. It is hoped that a systematic study of such data will provide a more definite answer to the question of whether radar cross section measurements are of potential diagnostic value. Further, such questions as the diagnostic possibilities of bistatic radar, or the existence of scaling laws need to be investigated. Finally, more detailed attention should be paid to other aspects of the general backscatter problem, such as the anomalous scattering region which was reported by Wyatt[2] and confirmed by us.

VII. REFERENCES

1. Victorr A. Erma, Radar Cross Sections of Inhomogeneous Plasmas Spheres, Part I; Astrophysics Research Corporation Report, 2 April 1965.

2. Philip J. Wyatt, Applied Physics Letters, 6, 209, (1965).

FIG. 1
CASES I–A, B
$N = 4.189 \times 10^{24}$

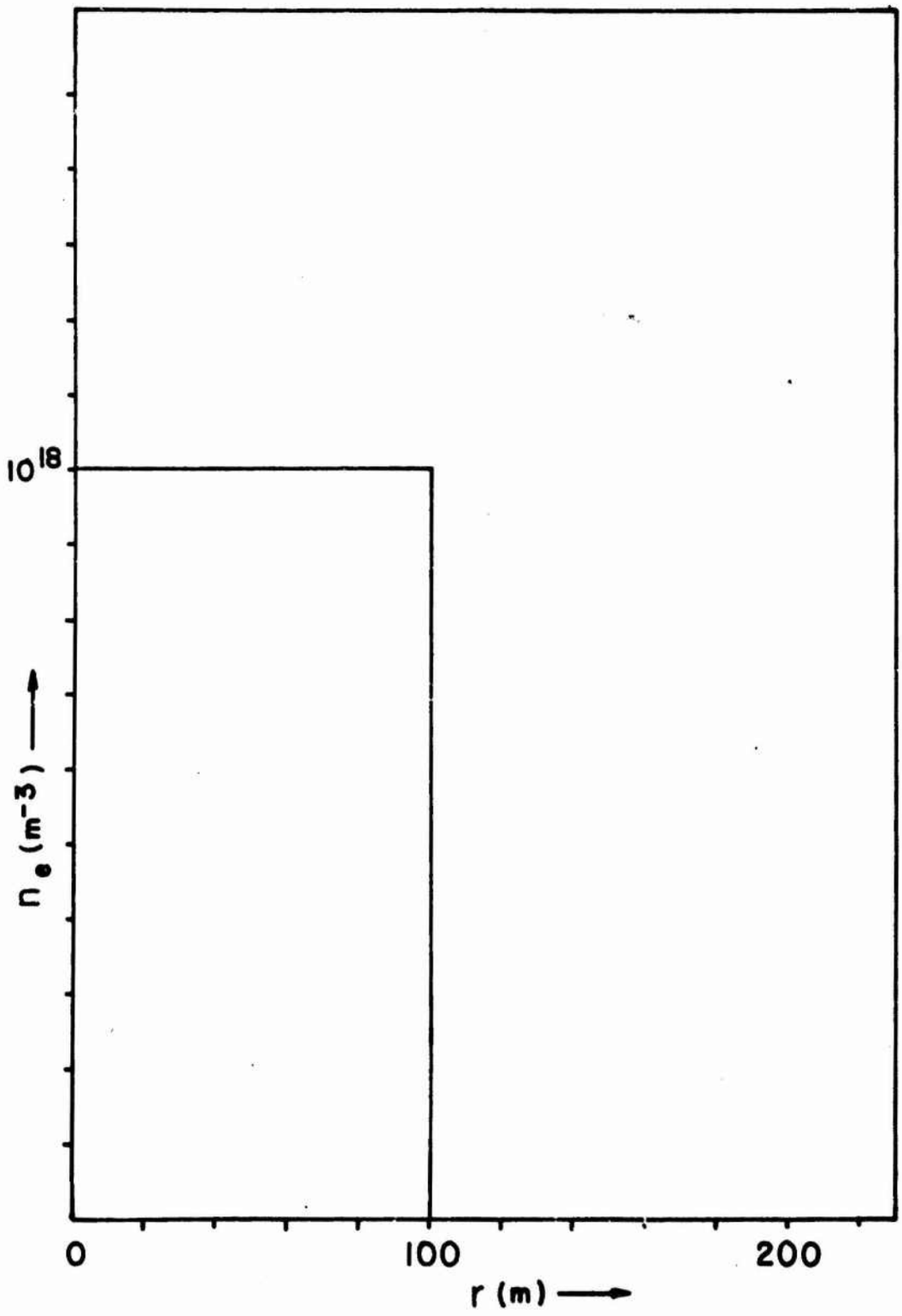

FIG. 2
CASE I–C
$N = 4.189 \times 10^{24}$

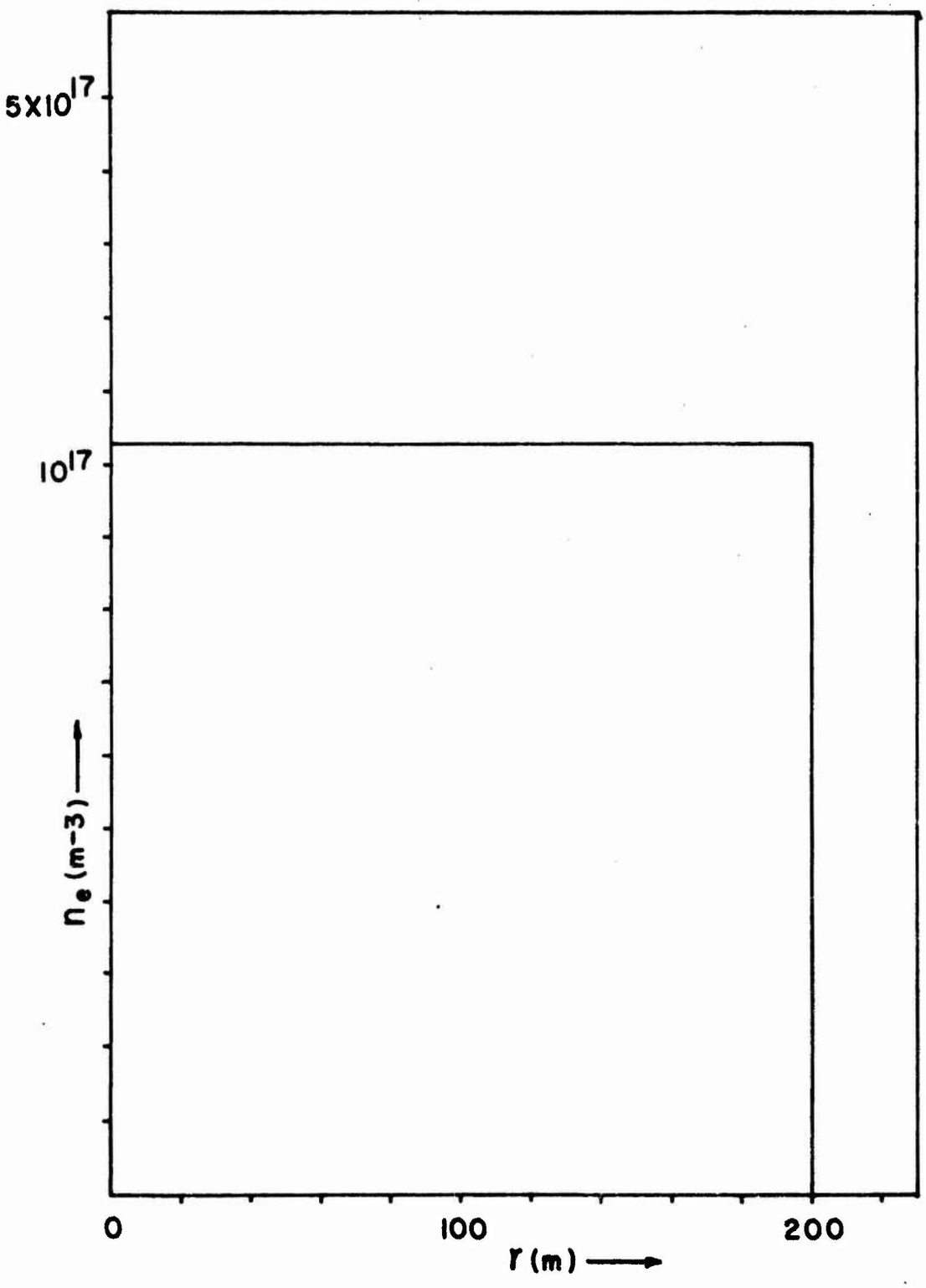

FIG. 3
CASE II-A
$N = 7.45 \times 10^{24}$

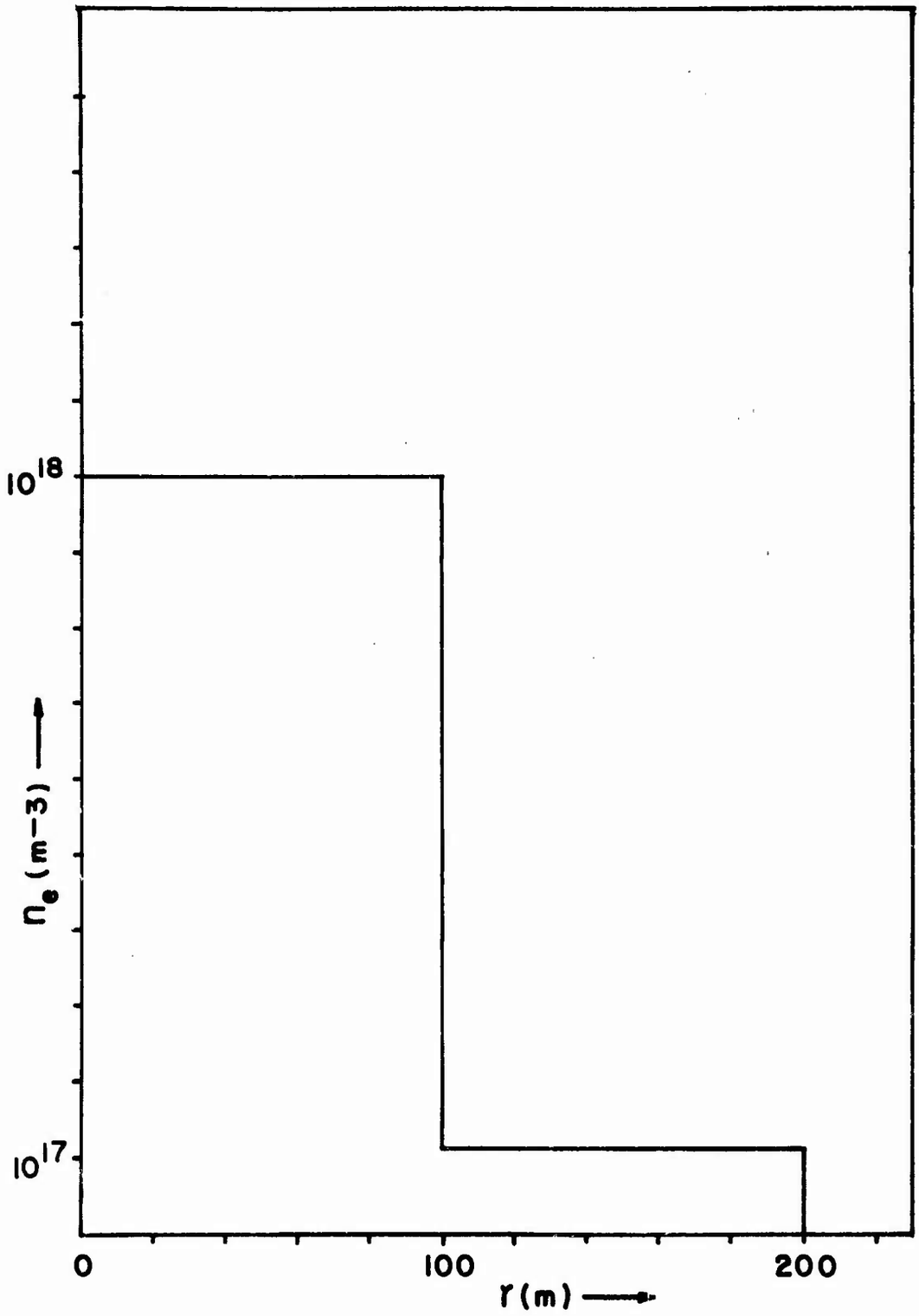

FIG. 4
CASE II–B
$N = 2.98 \times 10^{25}$

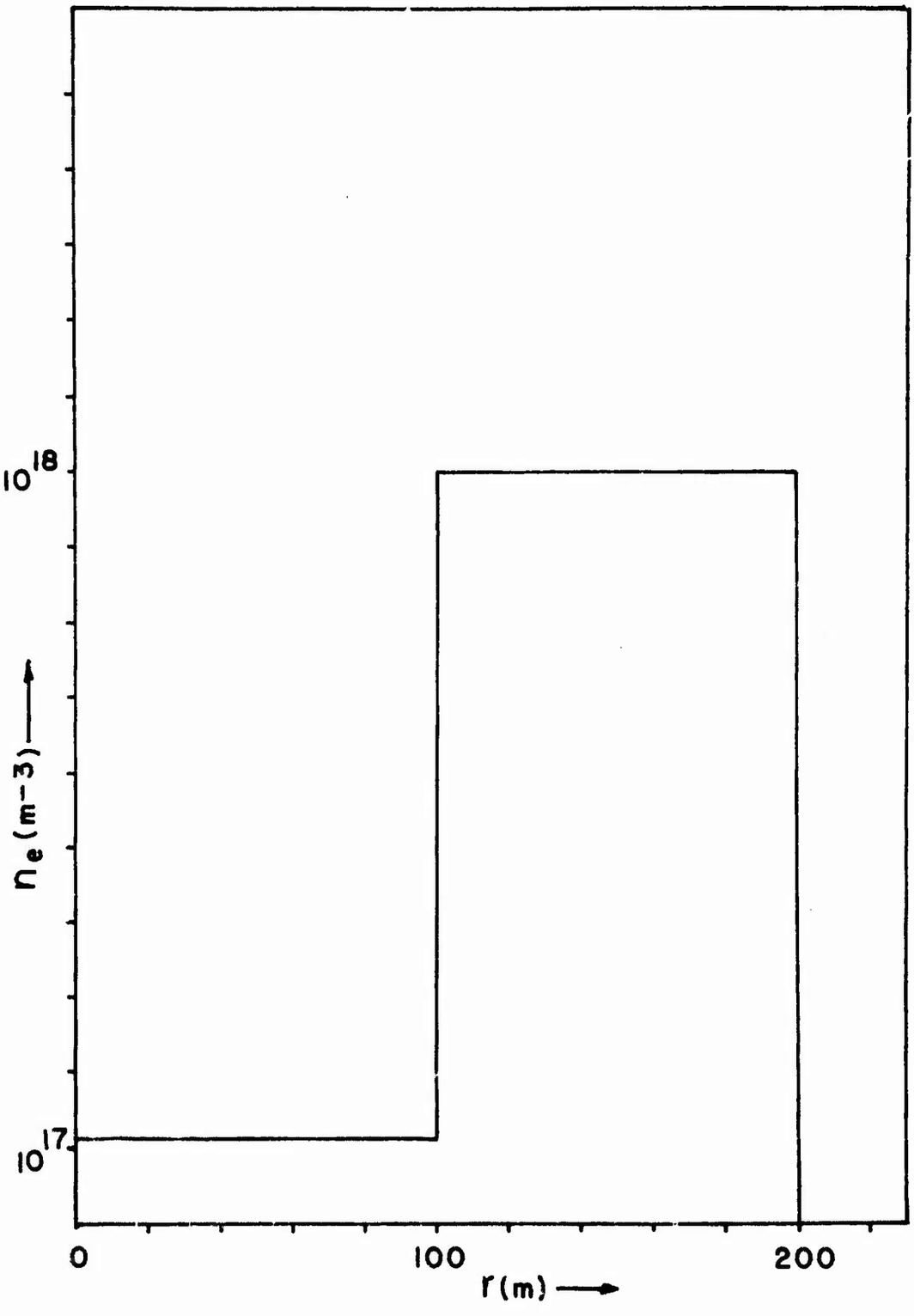

FIG. 5
CASE III–C
$N = 2.98 \times 10^{25}$

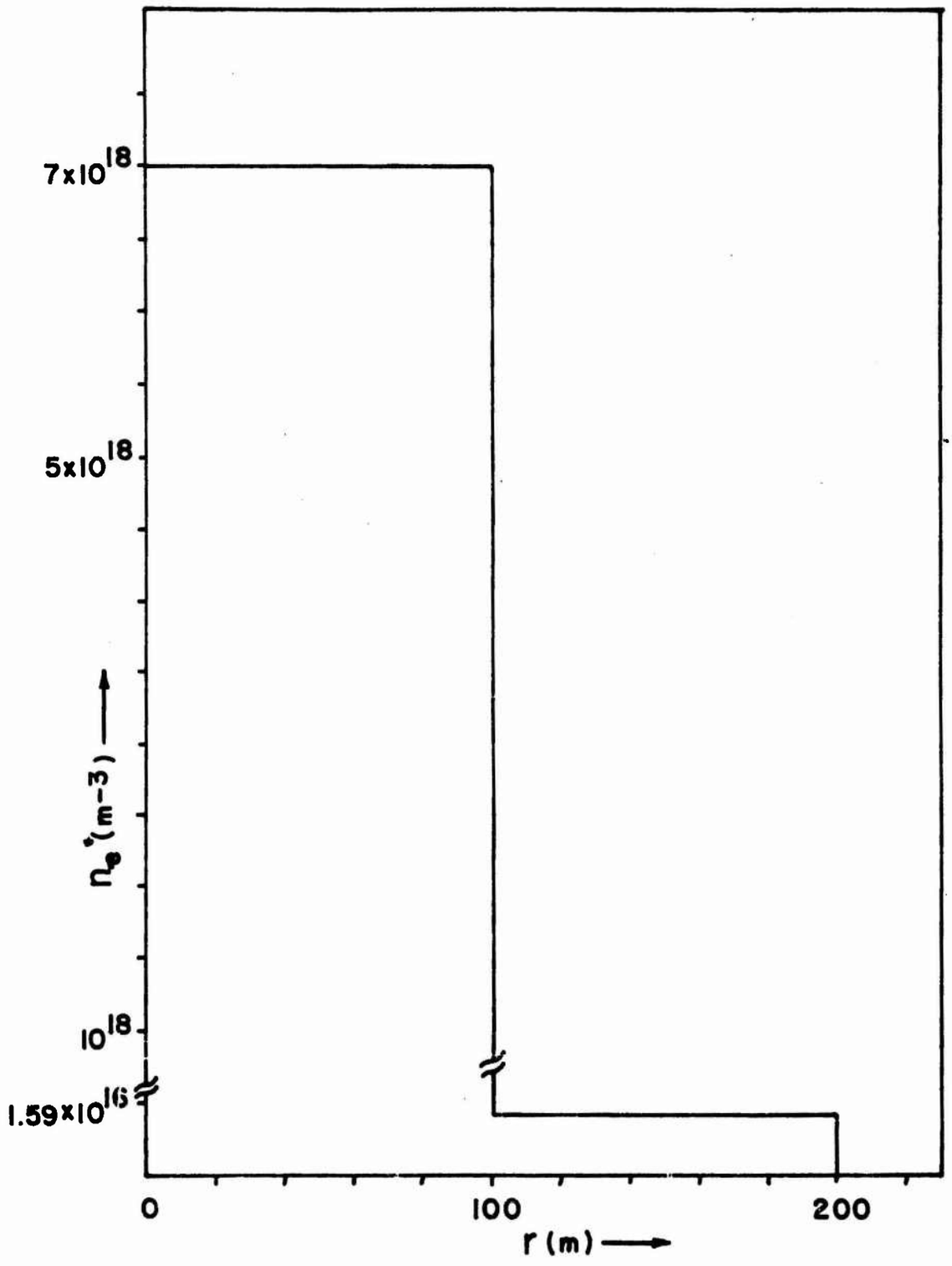

FIG. 6
CASE II – D
$N = 7.45 \times 10^{24}$

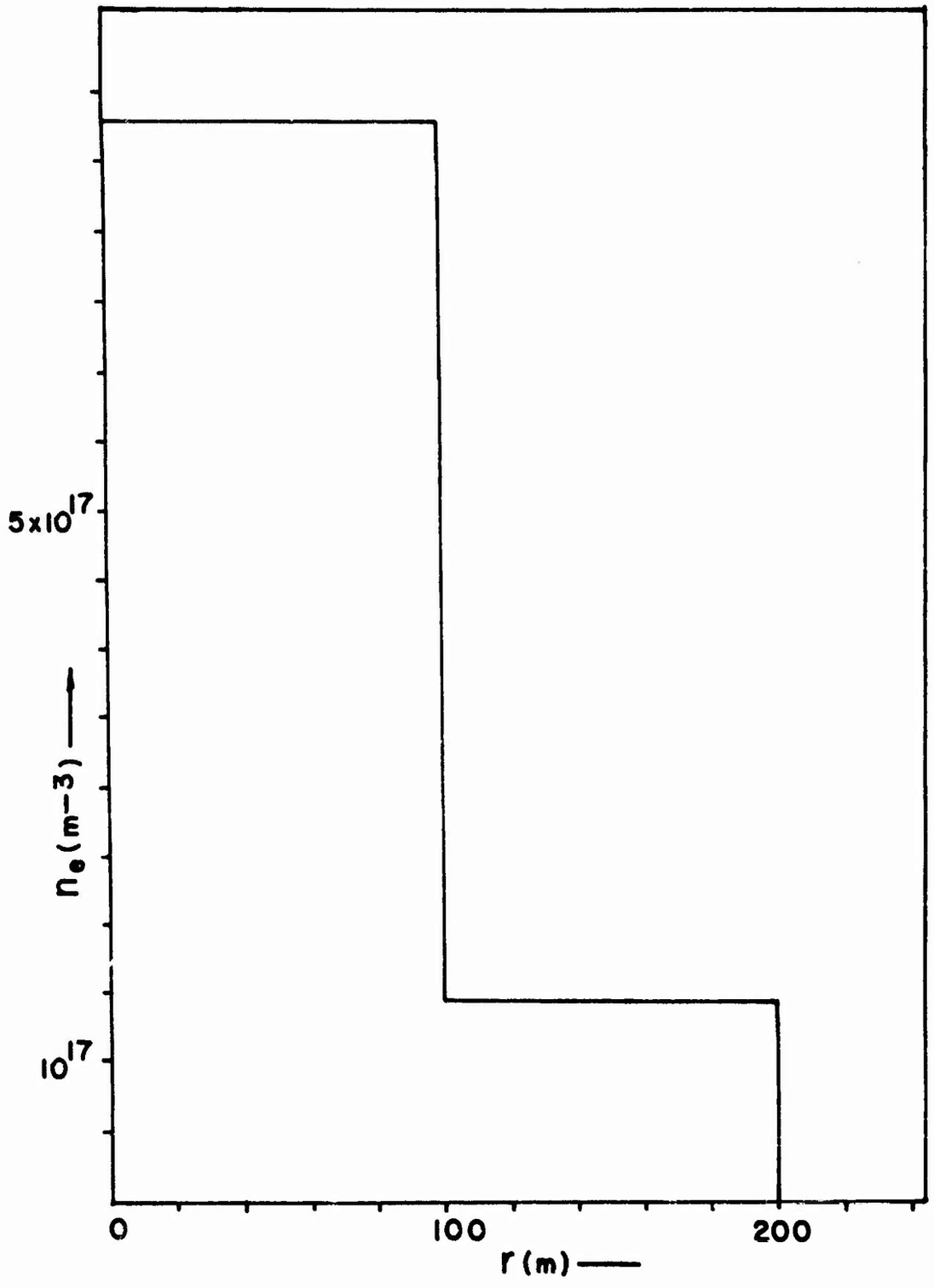

FIG. 7
CASE II–E
$N = 4.189 \times 10^{24}$

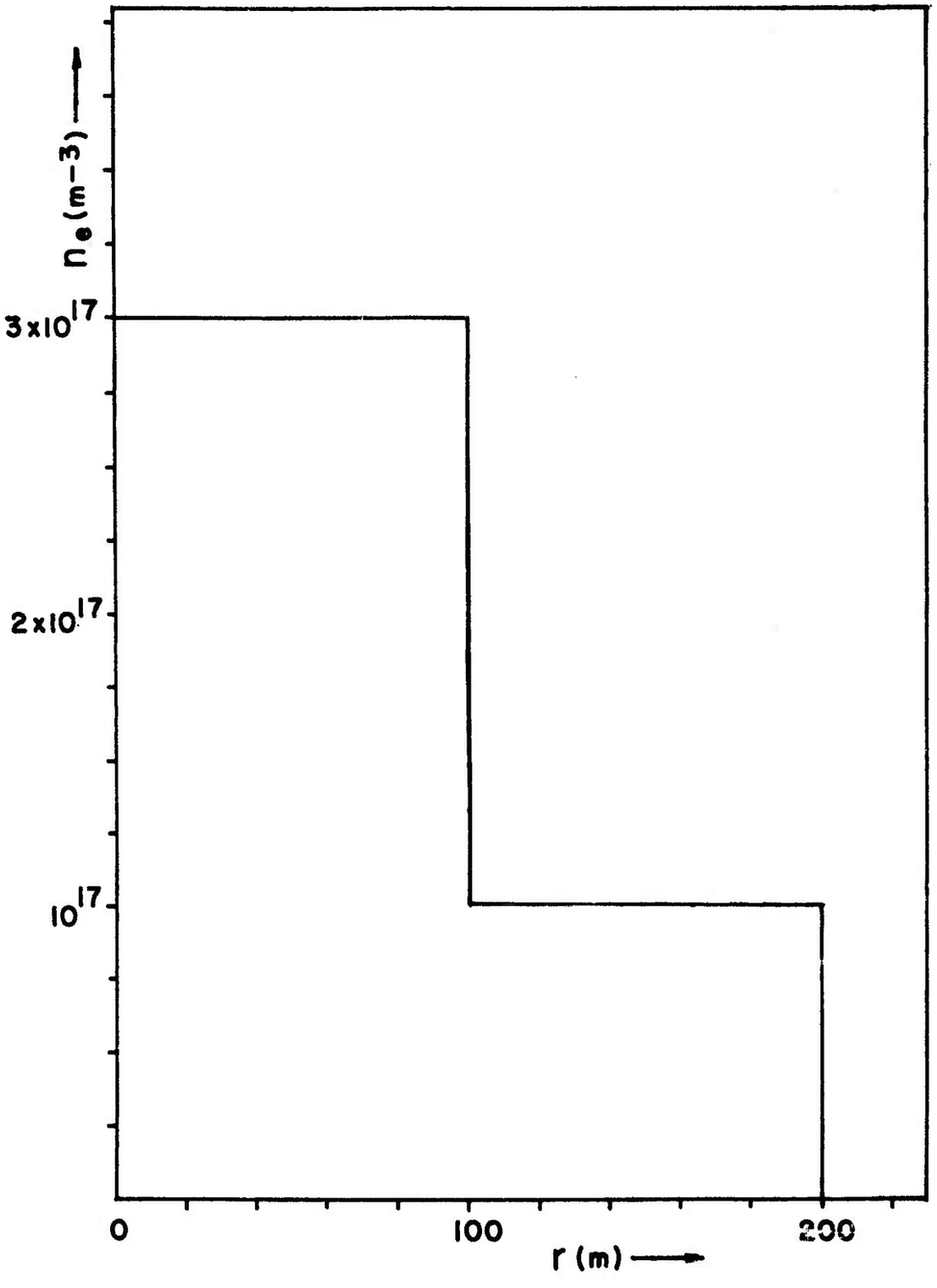

FIG. 8
CASE II – F
$N = 4.189 \times 10^{24}$

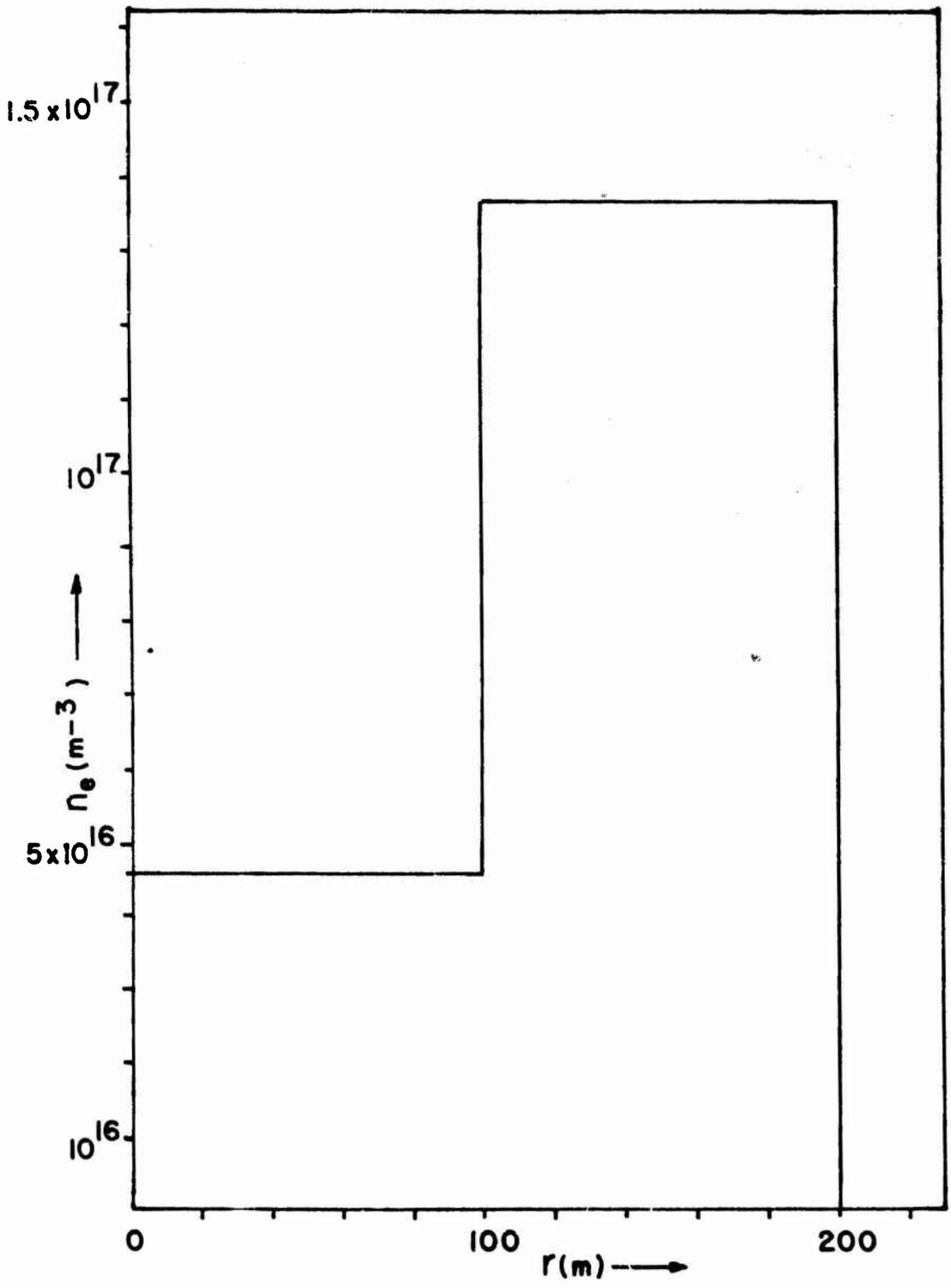

FIG. 9
CASE III-A
$N = 1.68 \times 10^{25}$

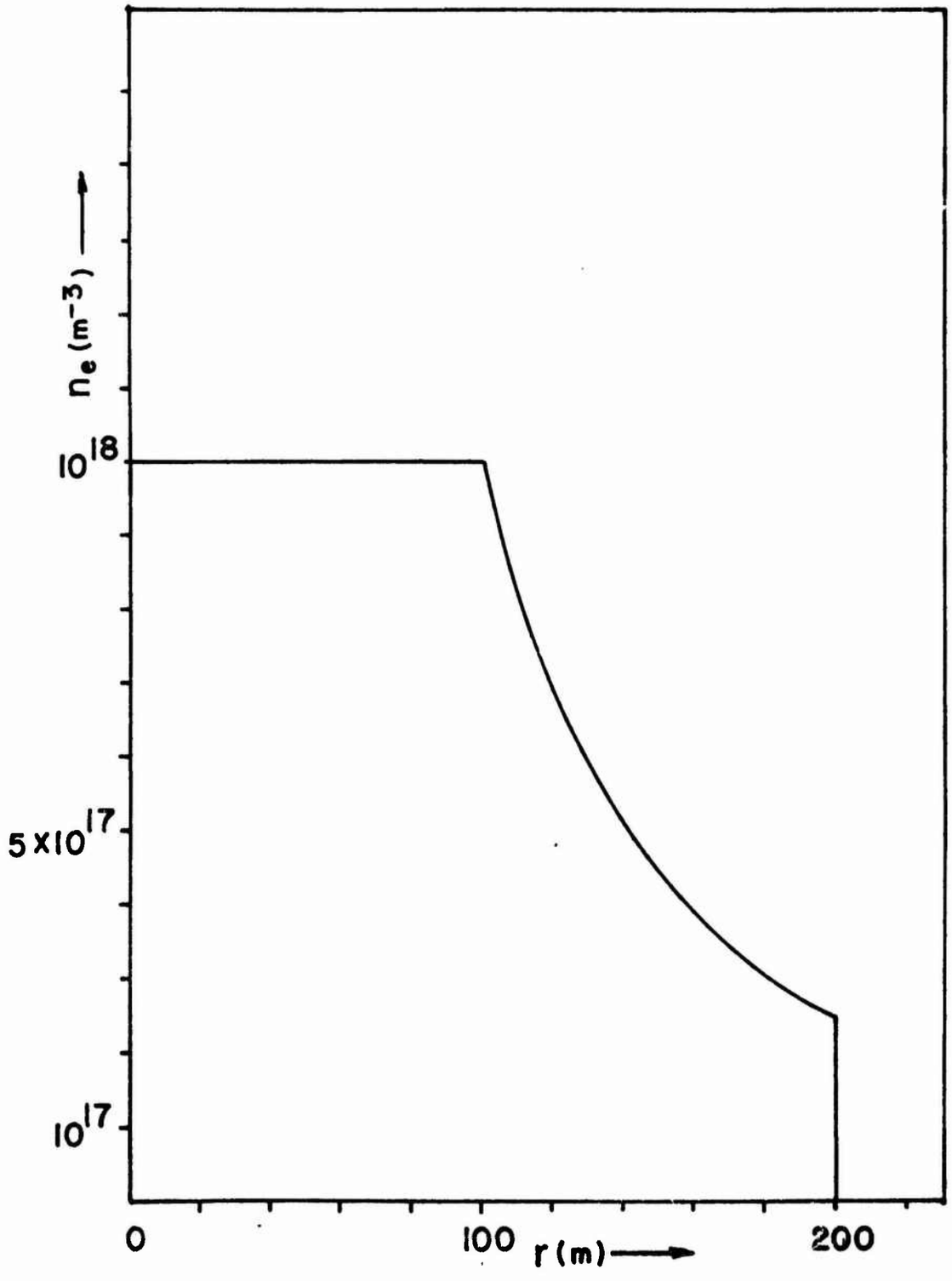

FIG. 10
CASE III–B
$N = 4.189 \times 10^{24}$

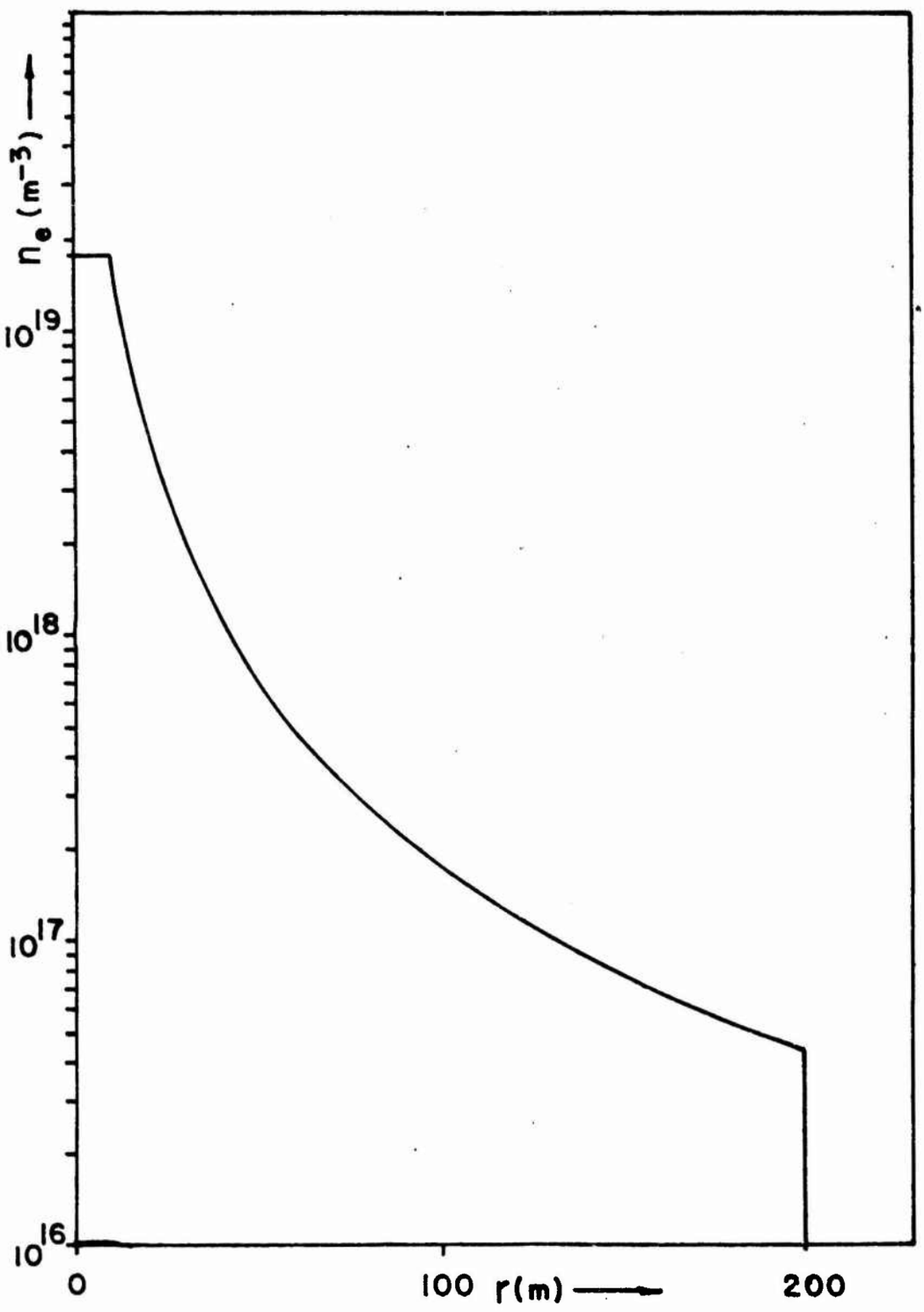

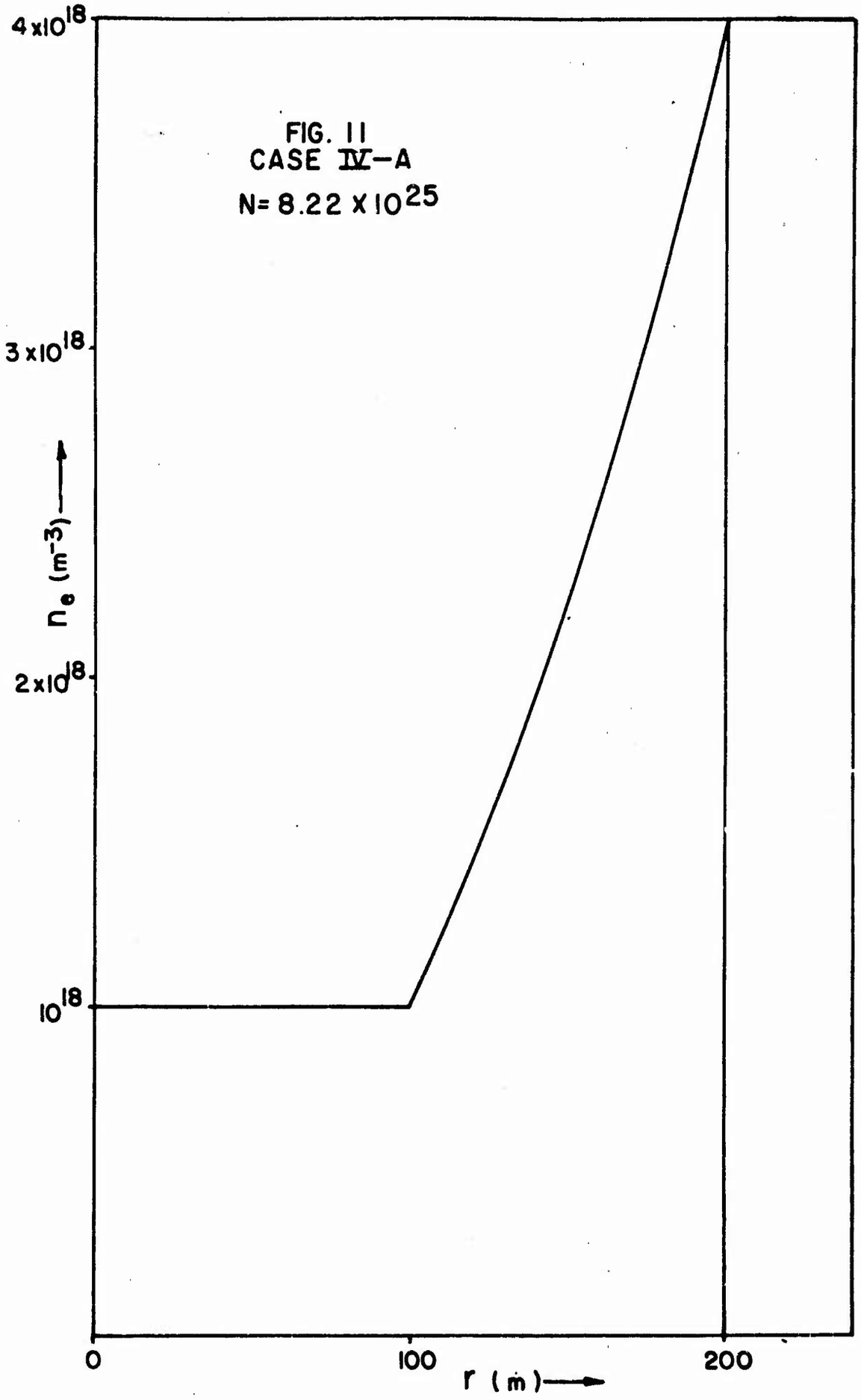

FIG. 11
CASE IV-A
$N = 8.22 \times 10^{25}$

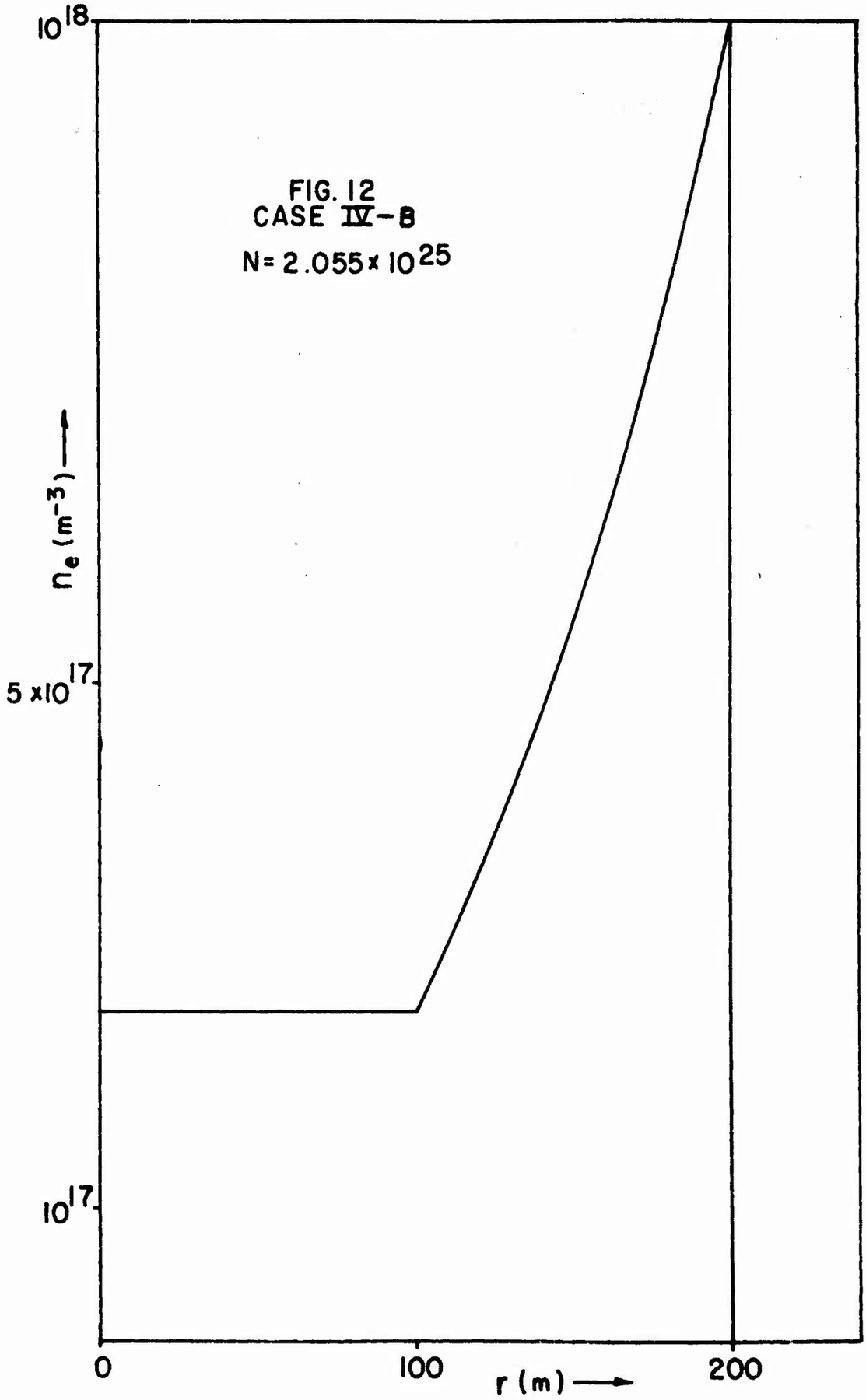

FIG. 12
CASE IV-B
$N = 2.055 \times 10^{25}$

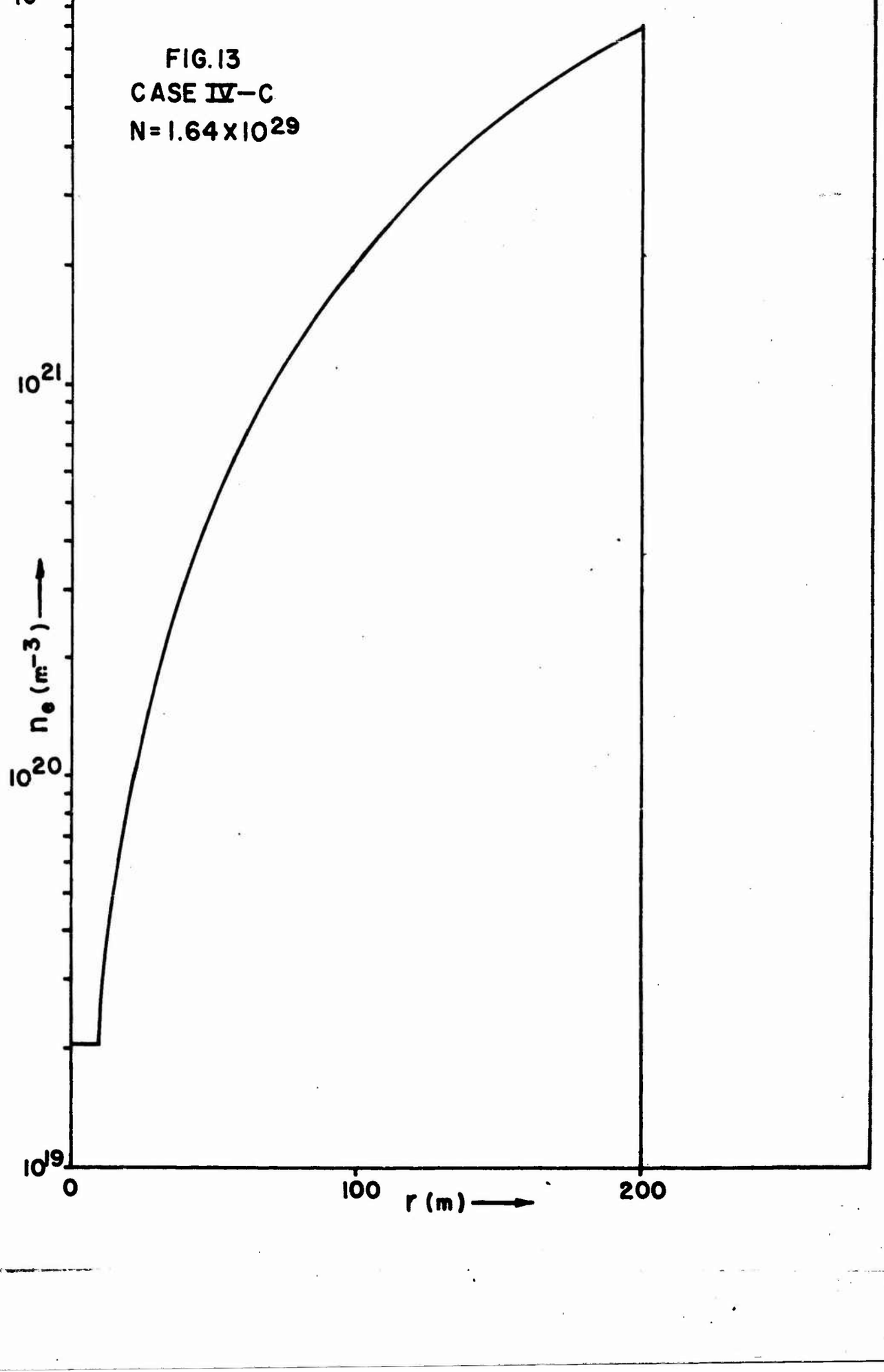
FIG. 13
CASE IV–C
N = 1.64 × 10^29
10^22
10^21
10^20
10^19
n_e (m^-3)
0
100
200
r (m)

FIG. 14
CASE IV-D
$N = 4.189 \times 10^{24}$

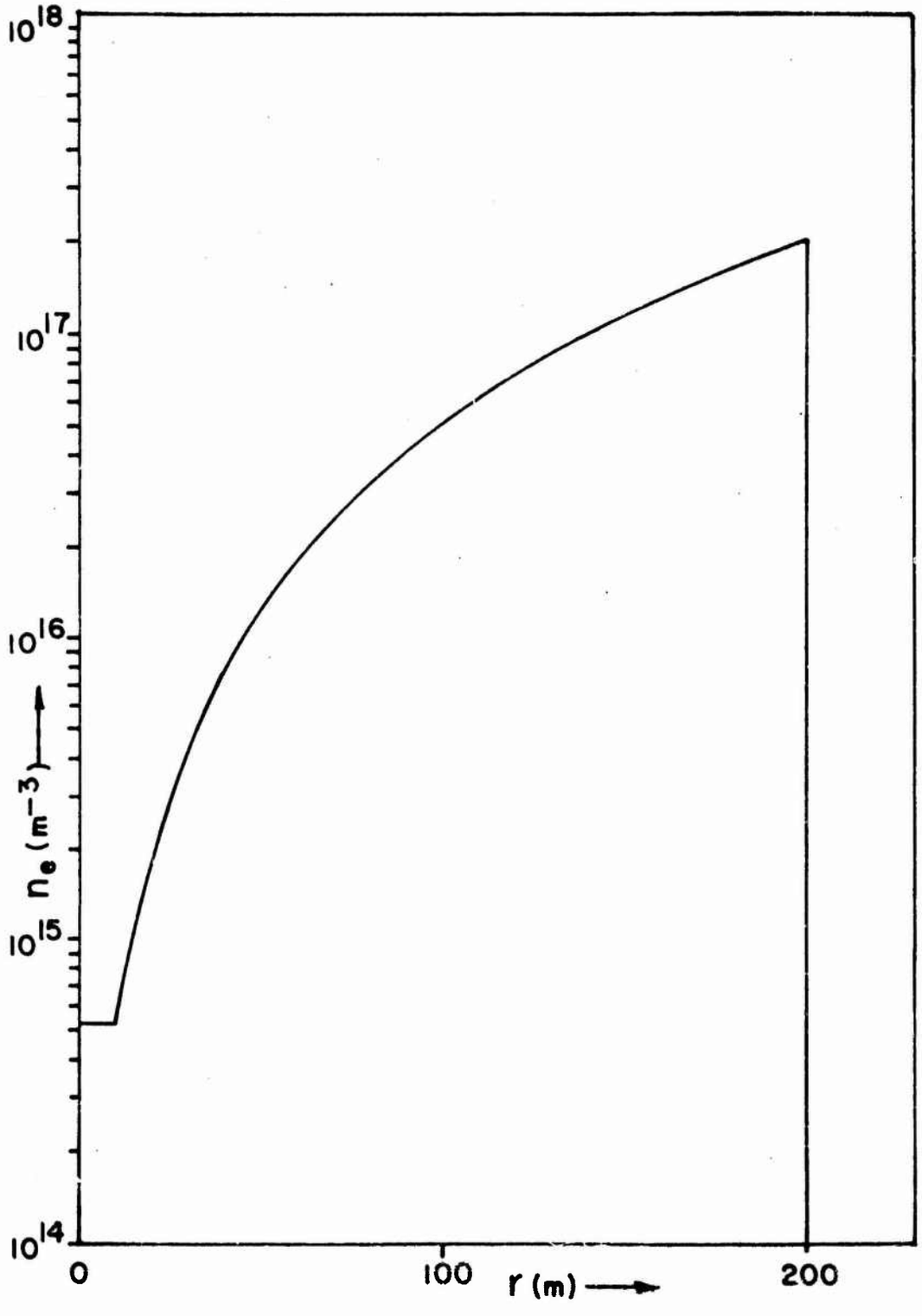

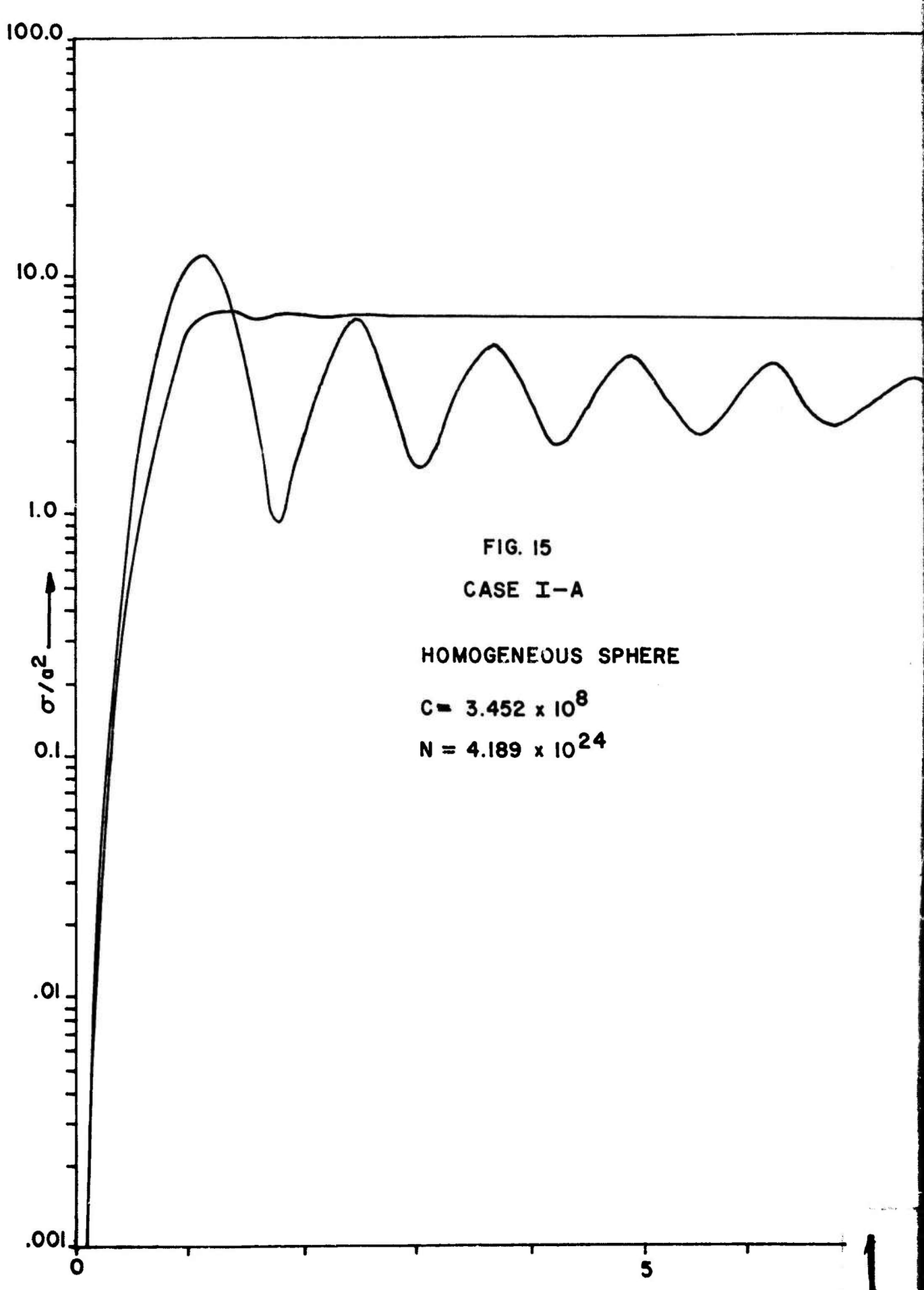

FIG. 15

CASE I–A

HOMOGENEOUS SPHERE

C = 3.452×10^{8}

N = 4.189×10^{24}

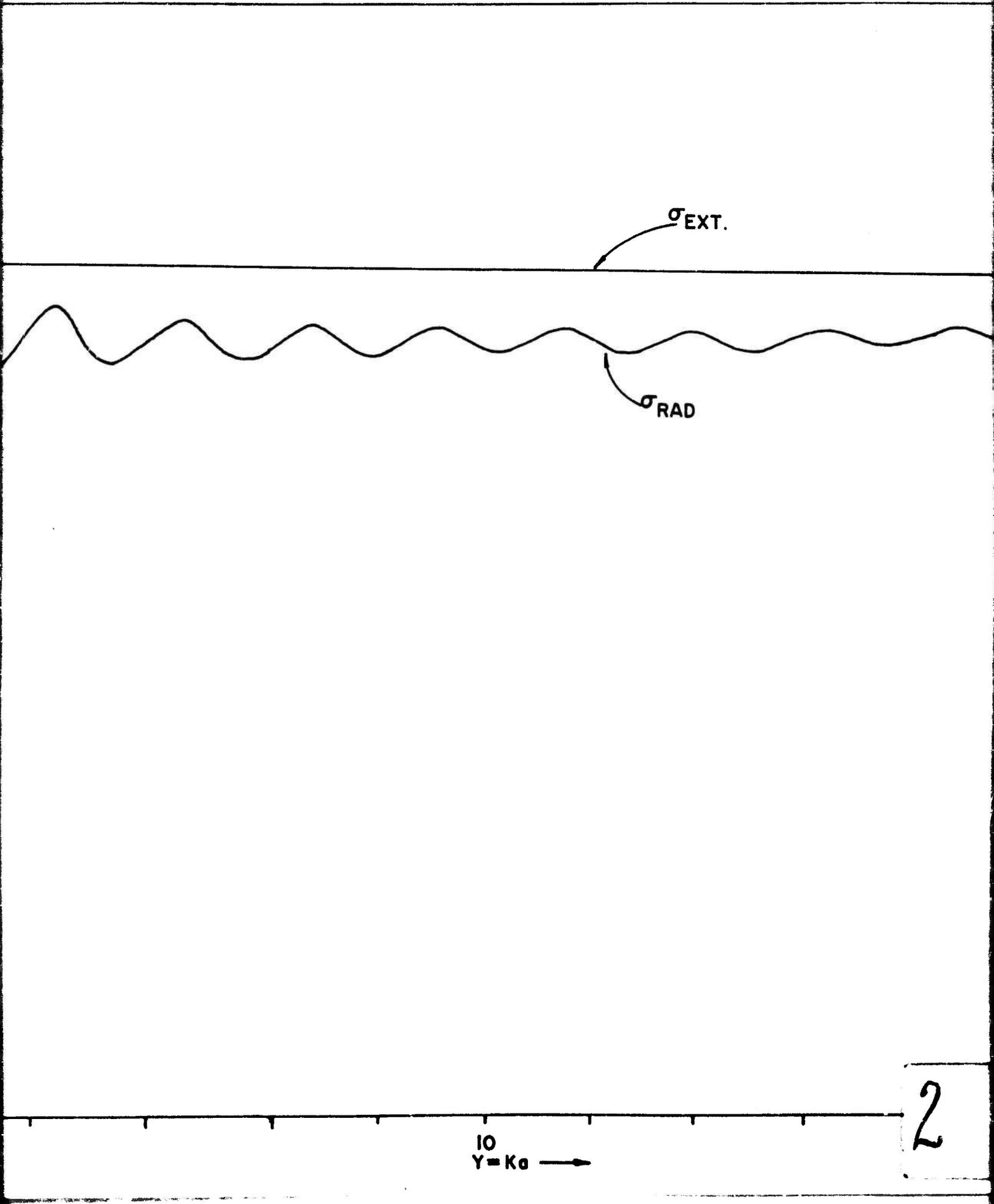
$\sigma_{EXT.}$
σ_{RAD}
10
Y = Ka

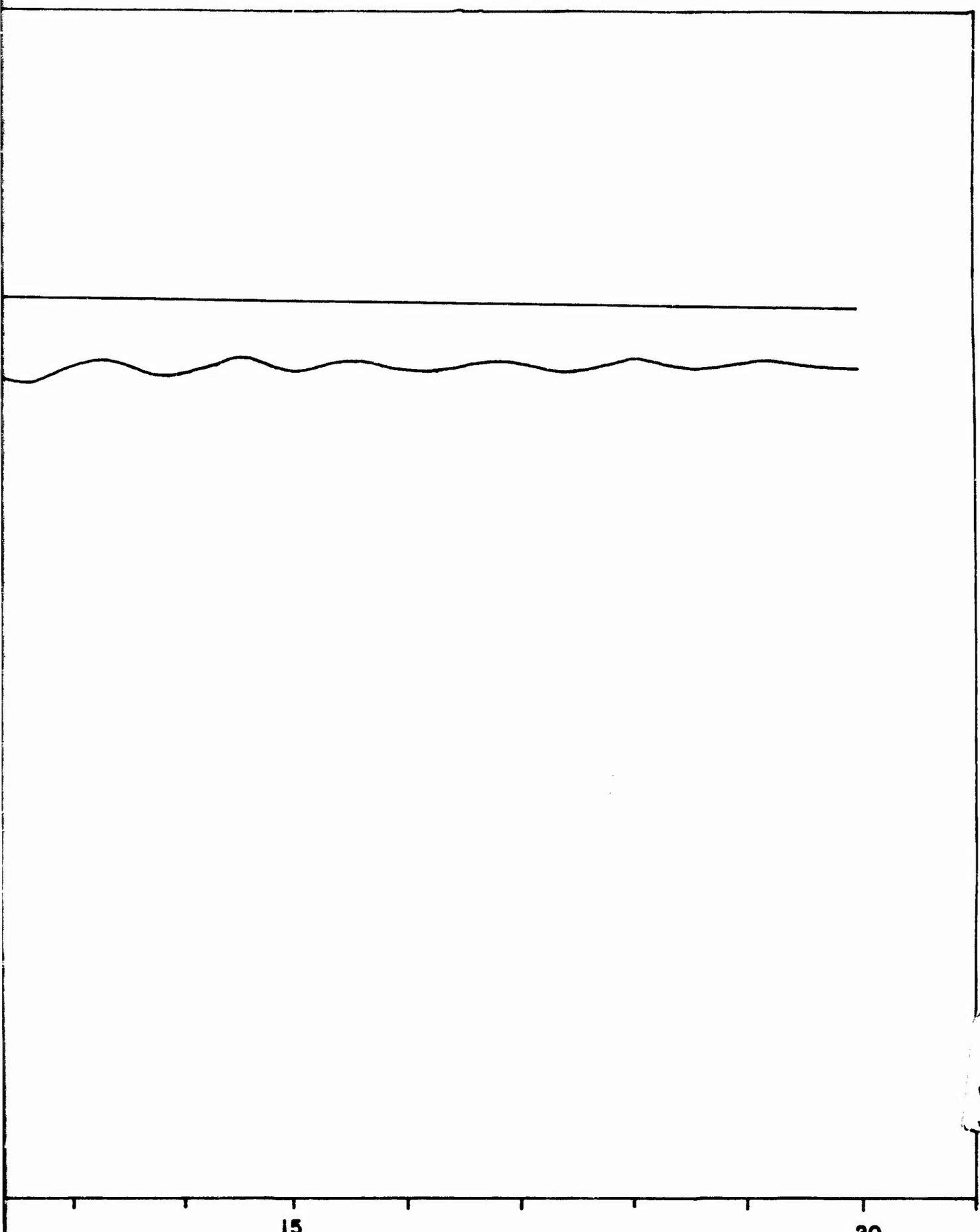

3

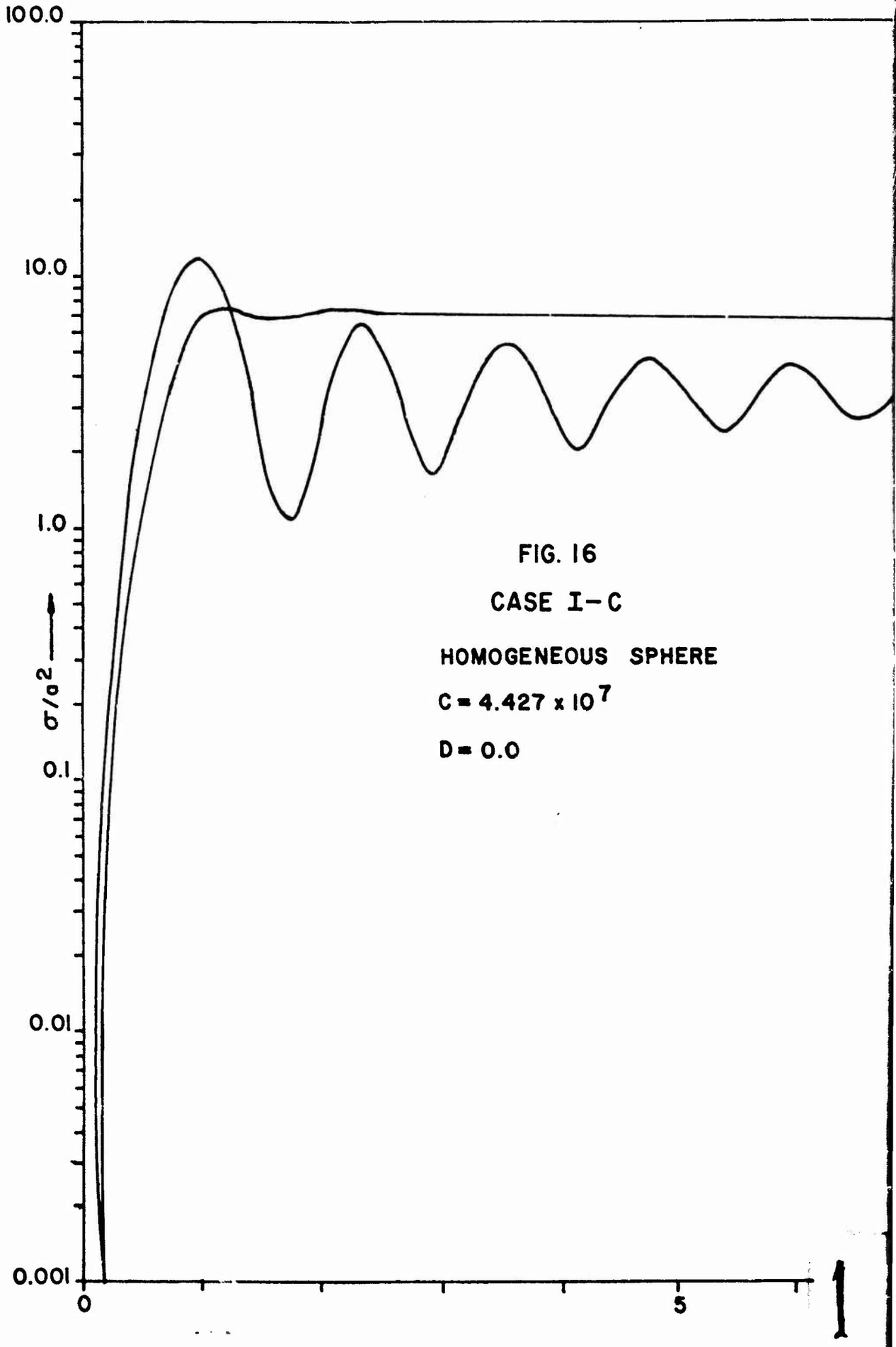
100.0
10.0
1.0
0.1
0.01
0.001
σ/a²
0
5
FIG. 16
CASE I-C
HOMOGENEOUS SPHERE
C = 4.427 x 10⁷
D = 0.0

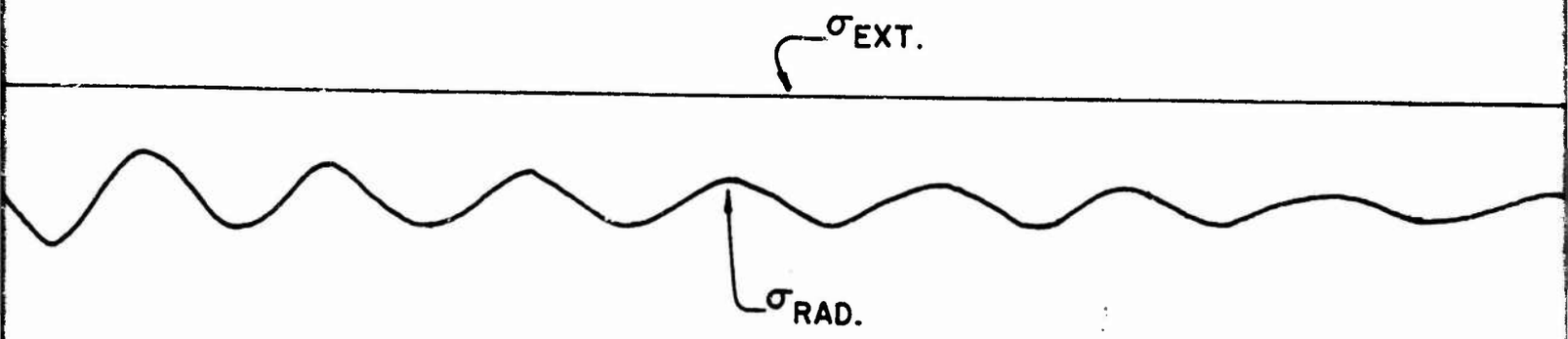

RE

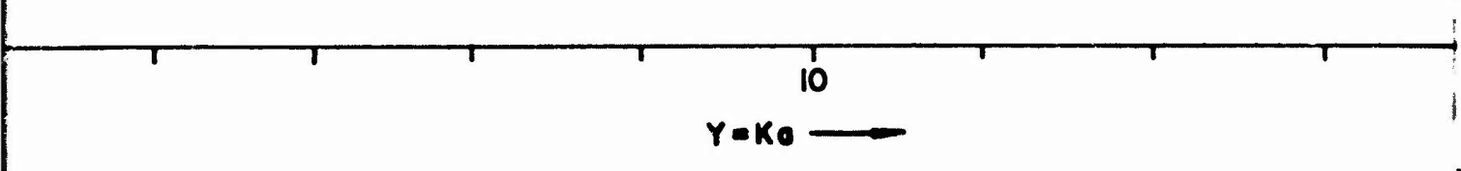

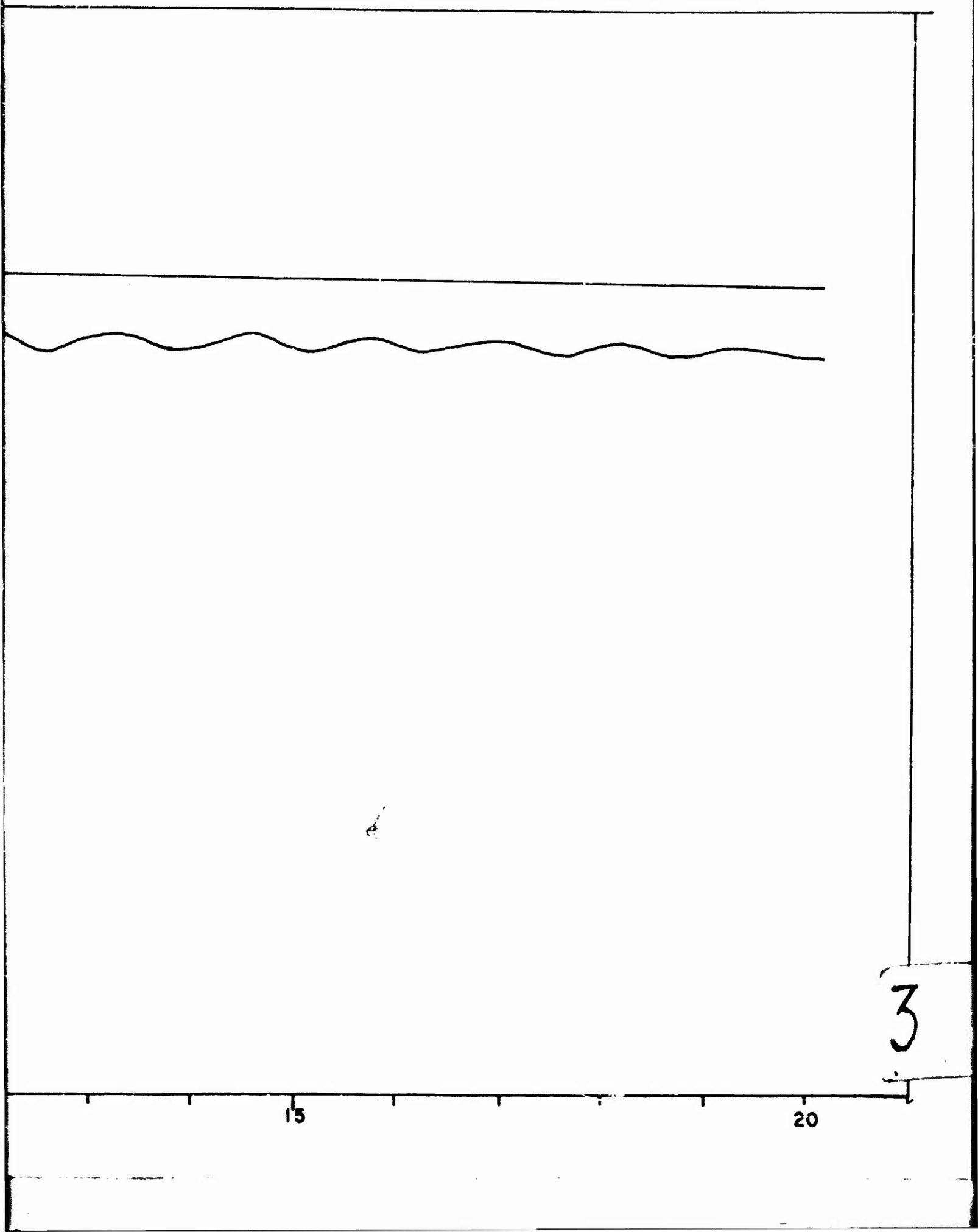
3
15
20

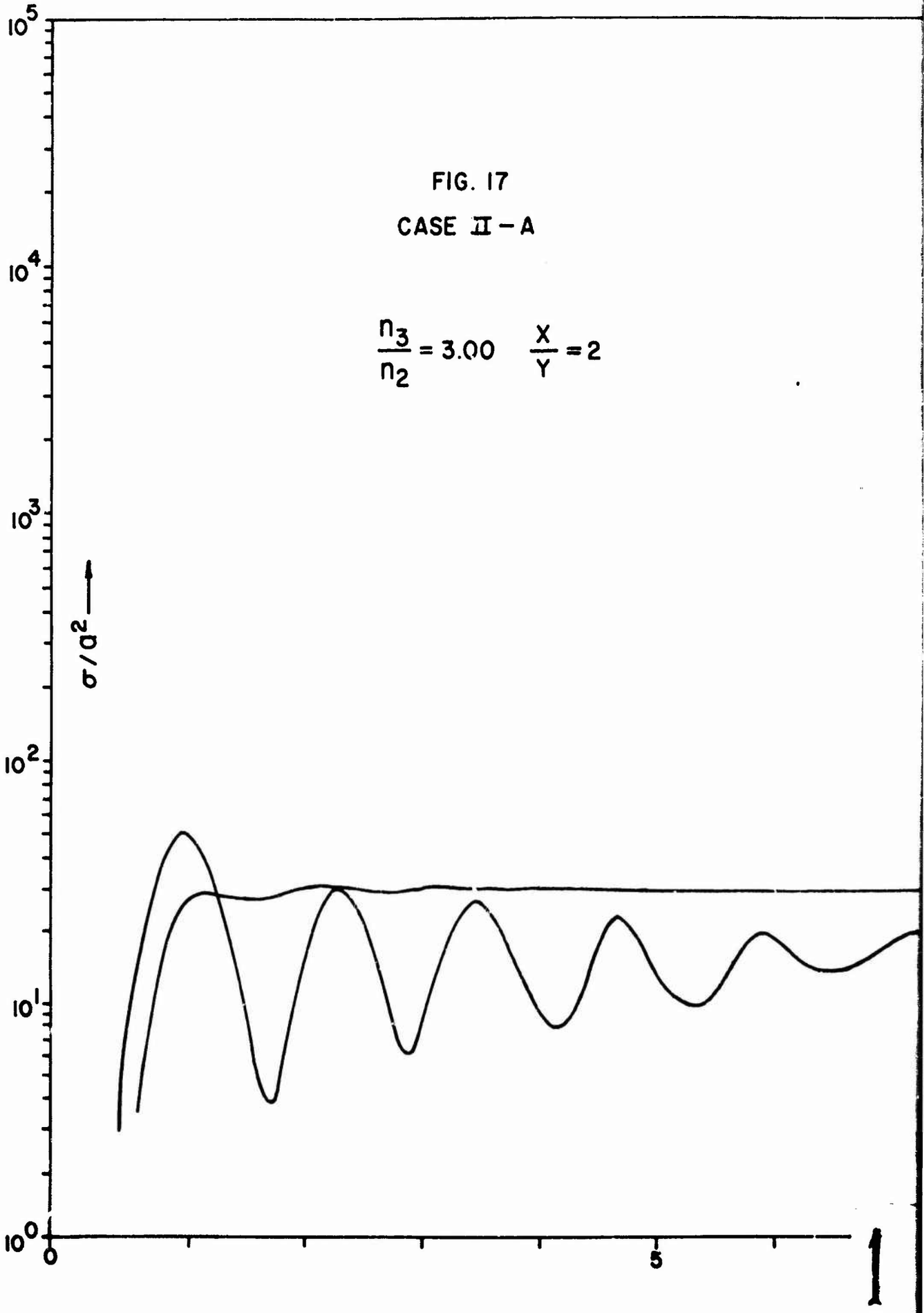
FIG. 17
CASE II – A
$\frac{n_3}{n_2} = 3.00 \quad \frac{X}{Y} = 2$
10^5
10^4
10^3
10^2
10^1
10^0
σ/a^2
0
5
1

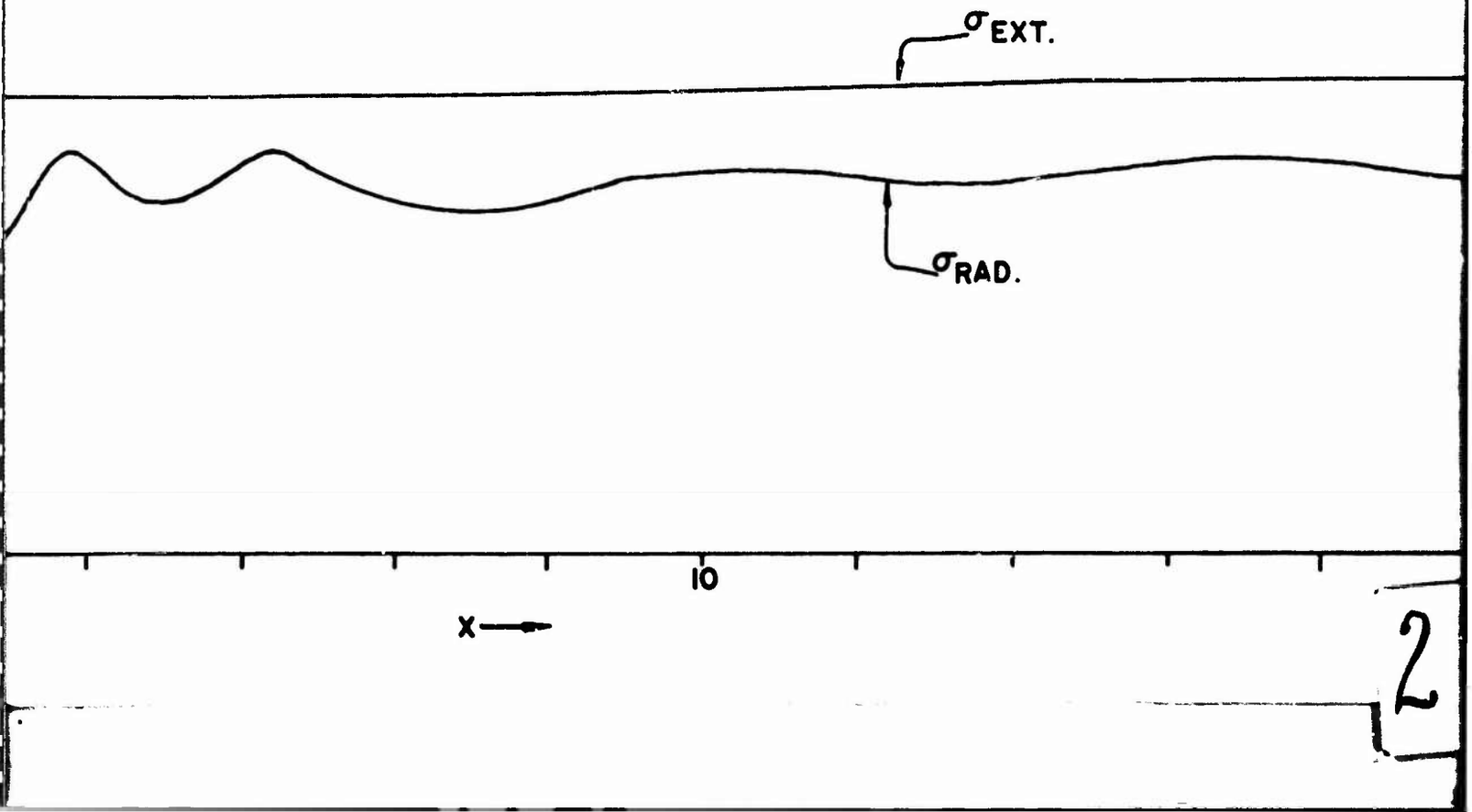
σ EXT.
σ RAD.
10
X

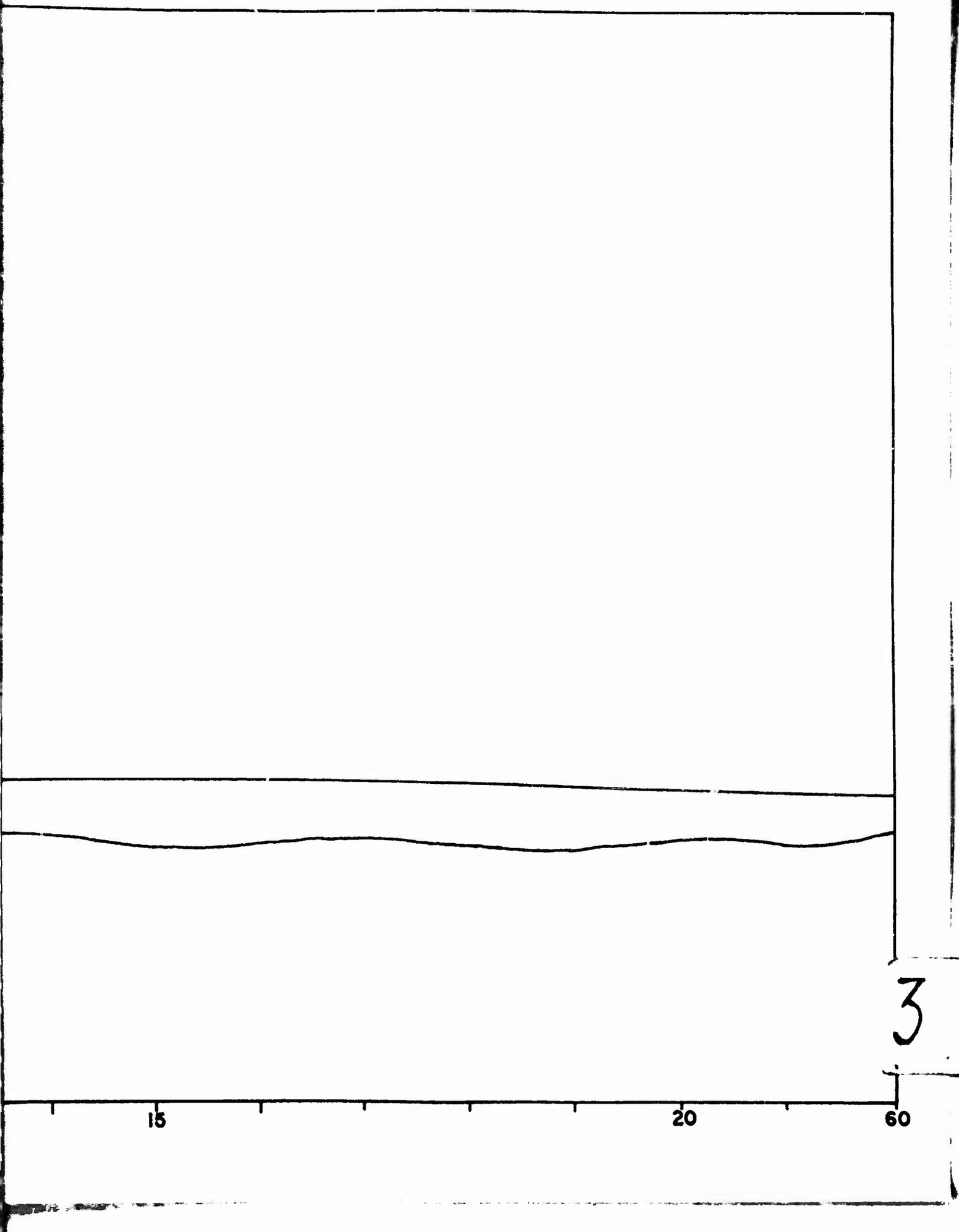
3
15
20
60

FIG. 18

CASE II–B

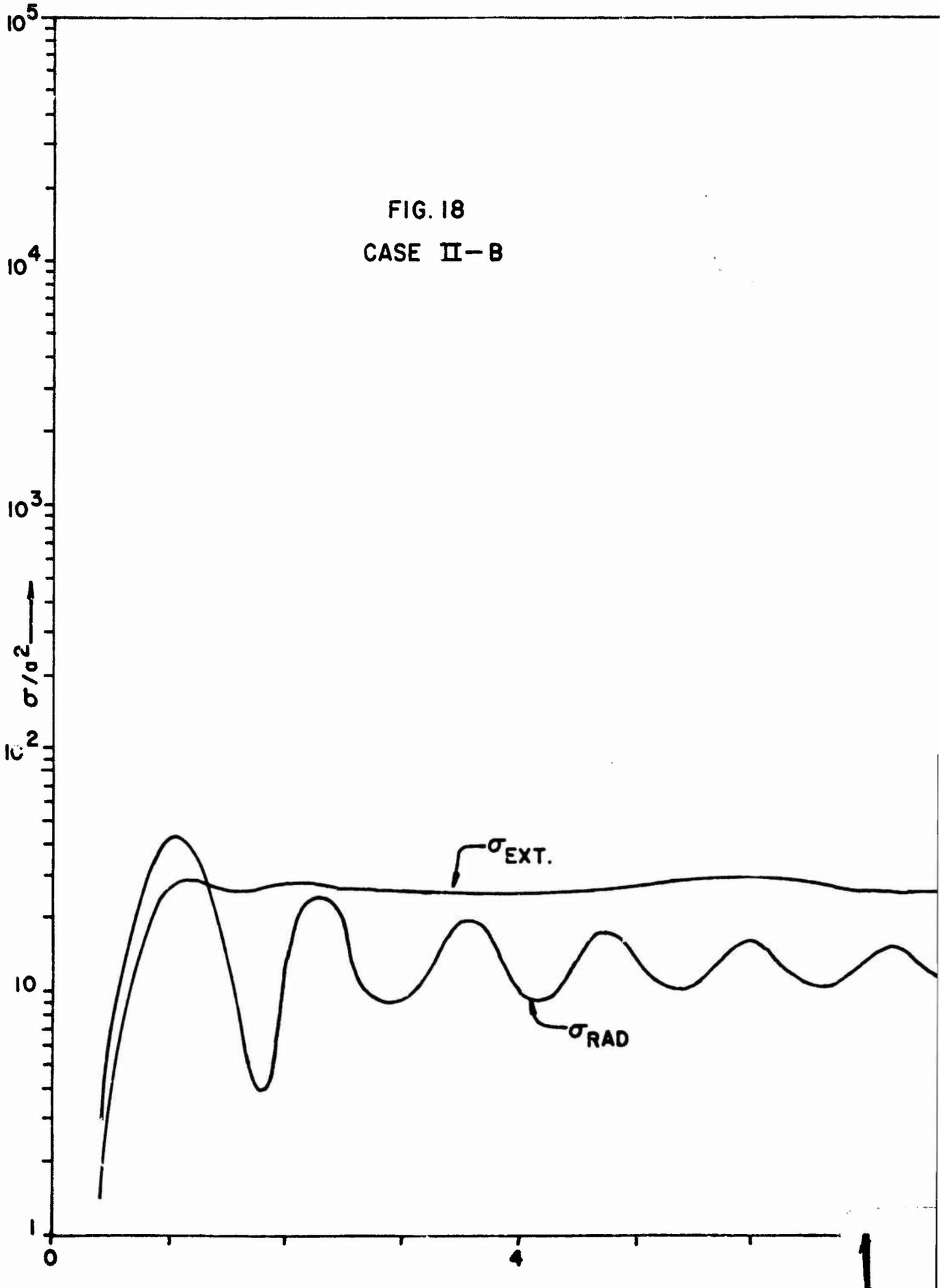

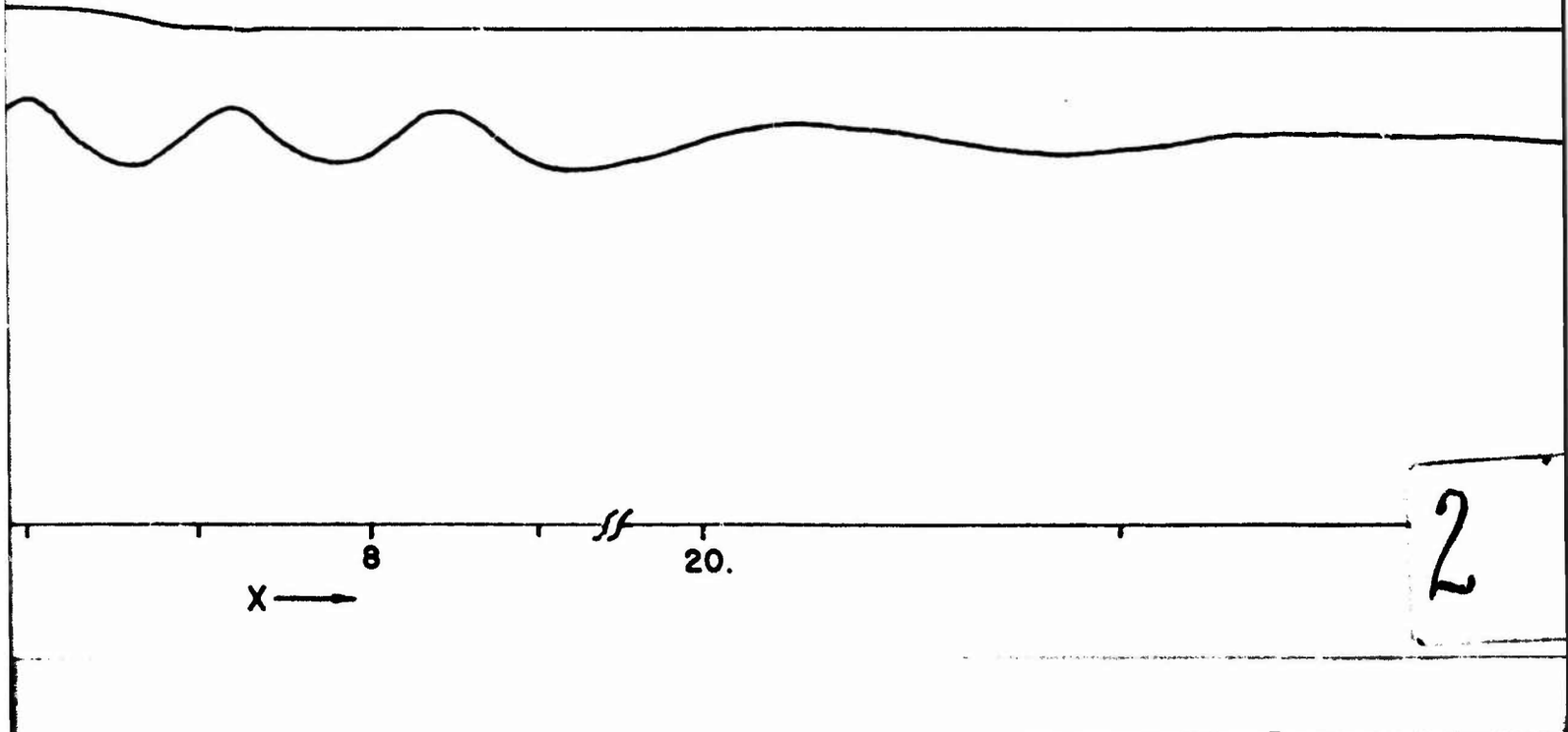
8
20.
X

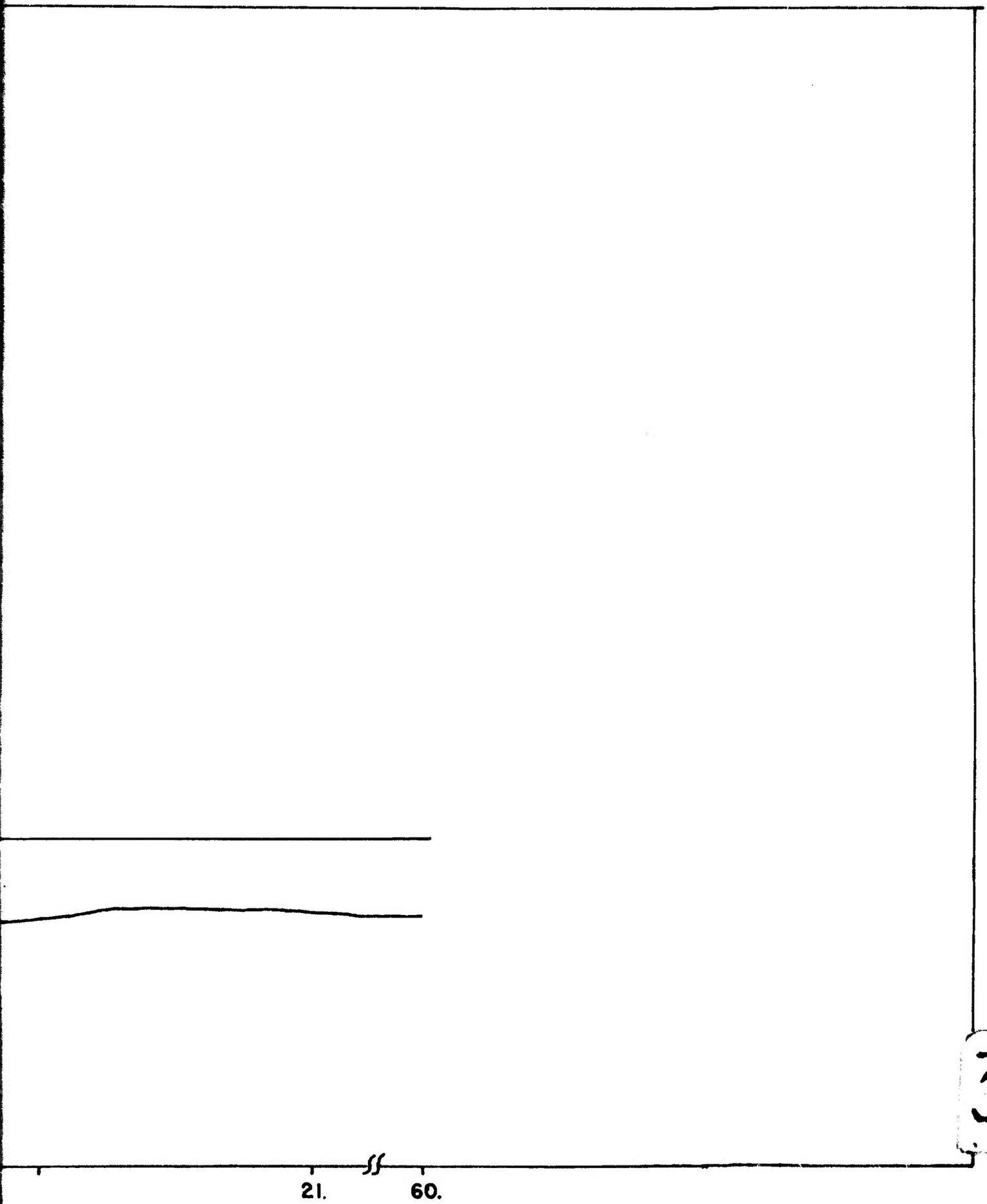
21.
60.

FIG. 19
CASE II — C

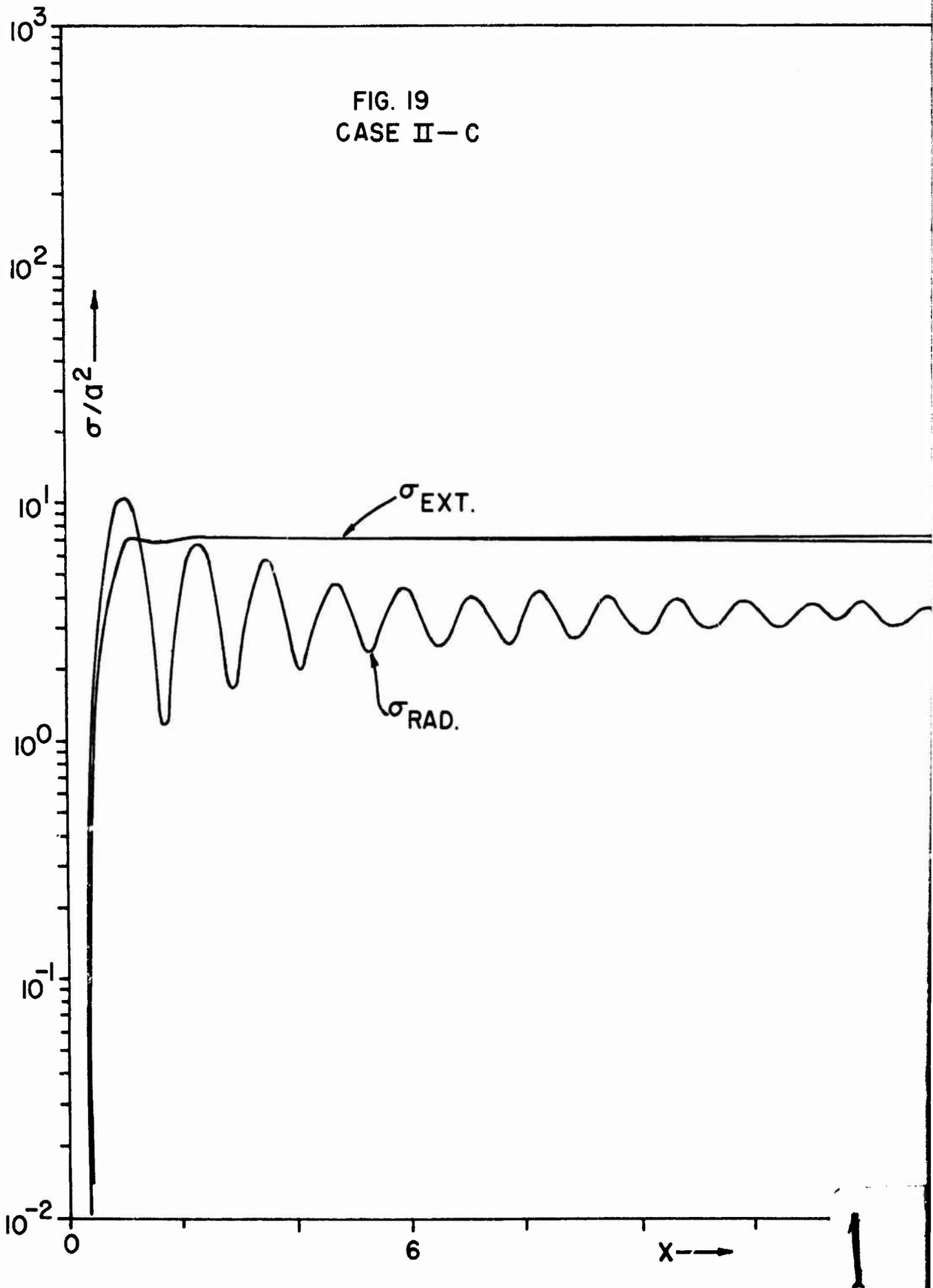

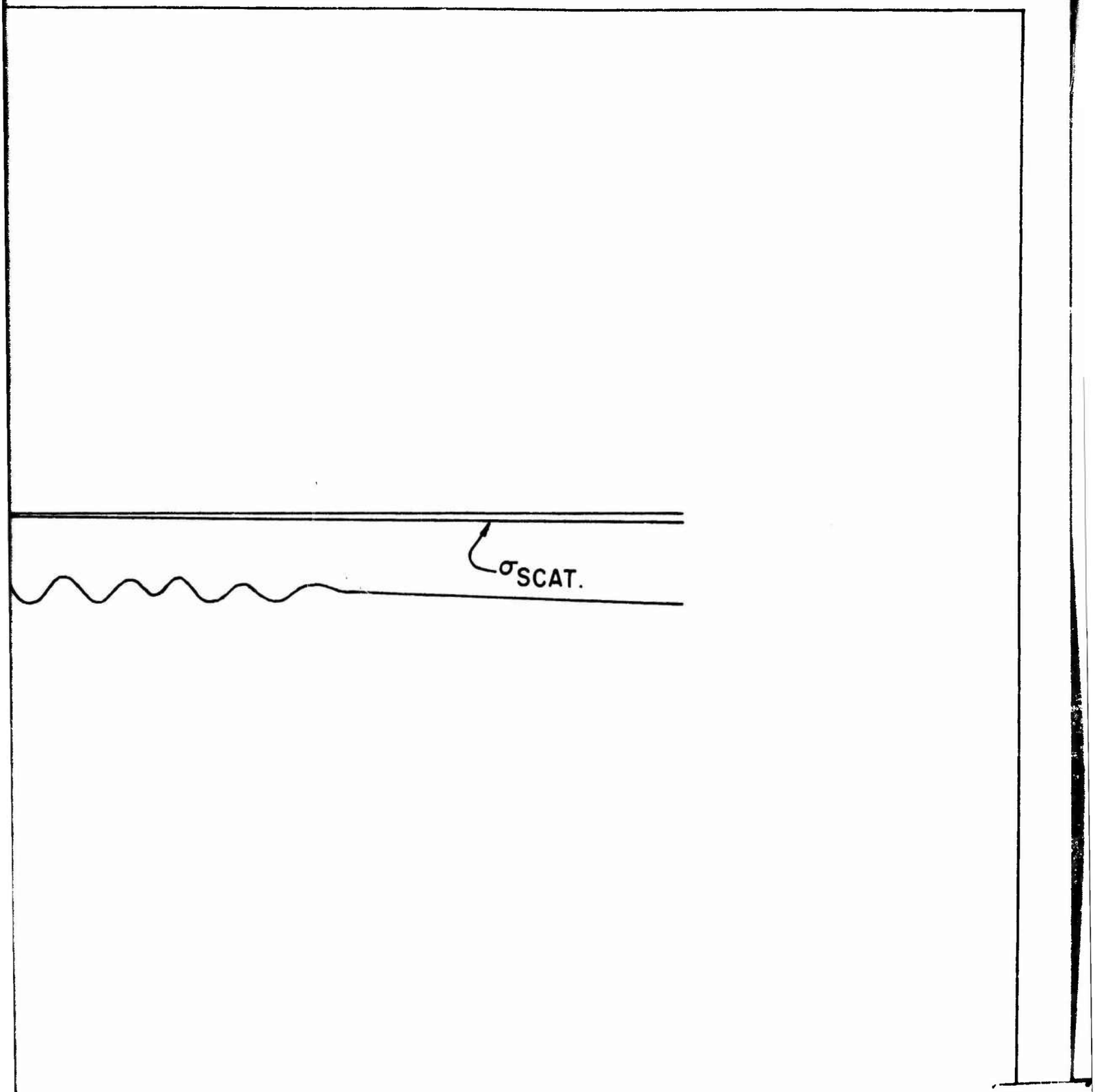
σSCAT.
14
20
30

FIG. 20
CASE II–D

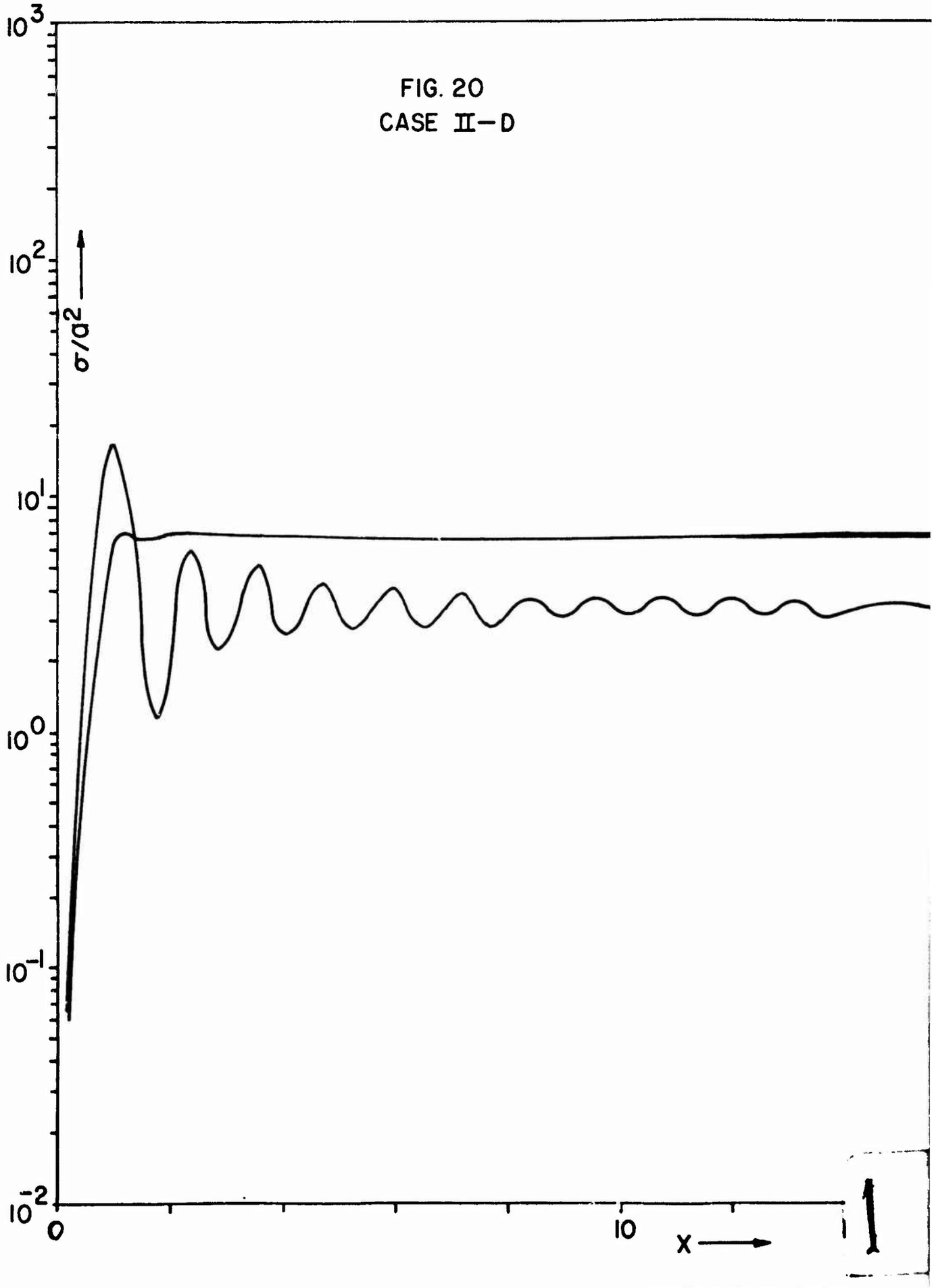

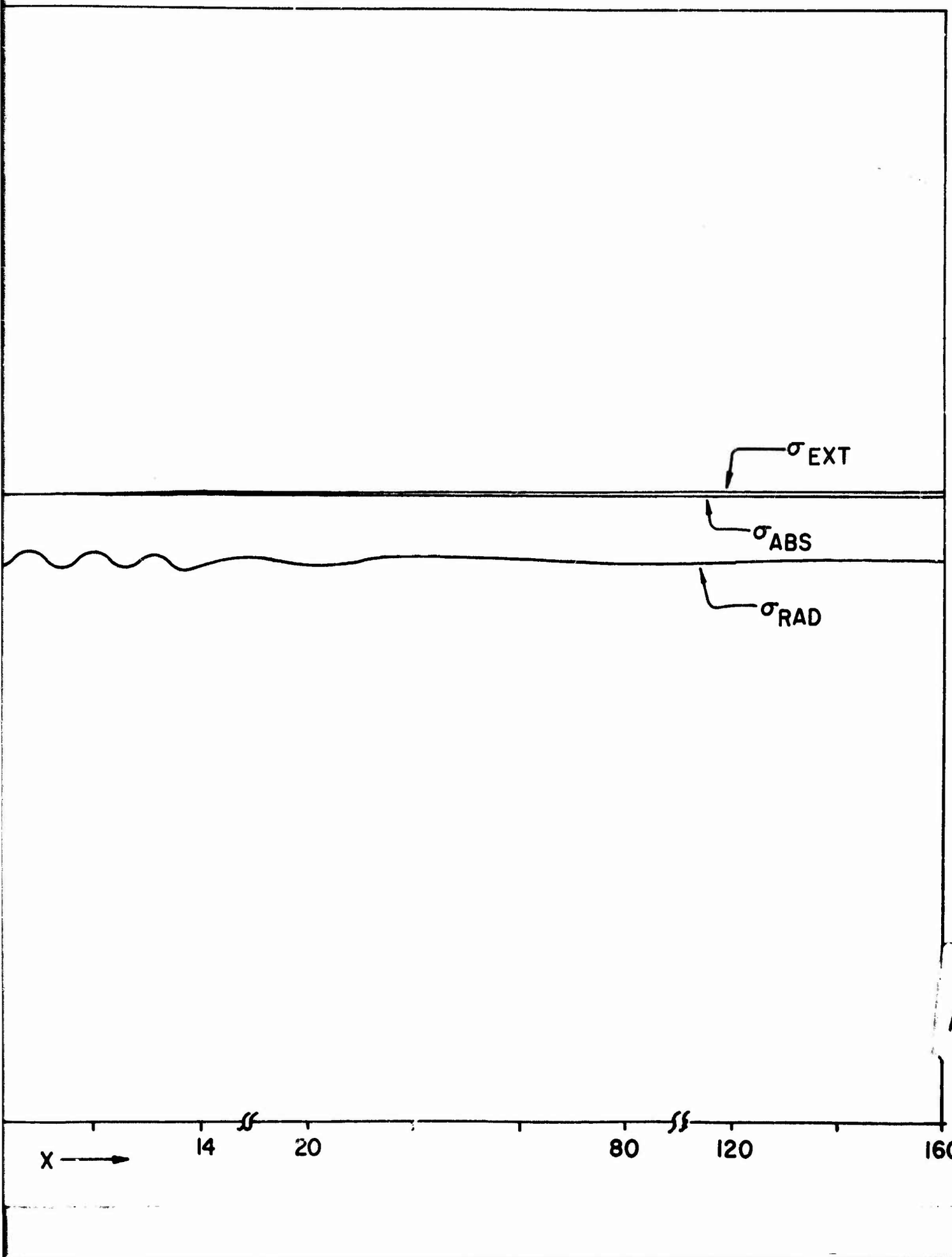

2

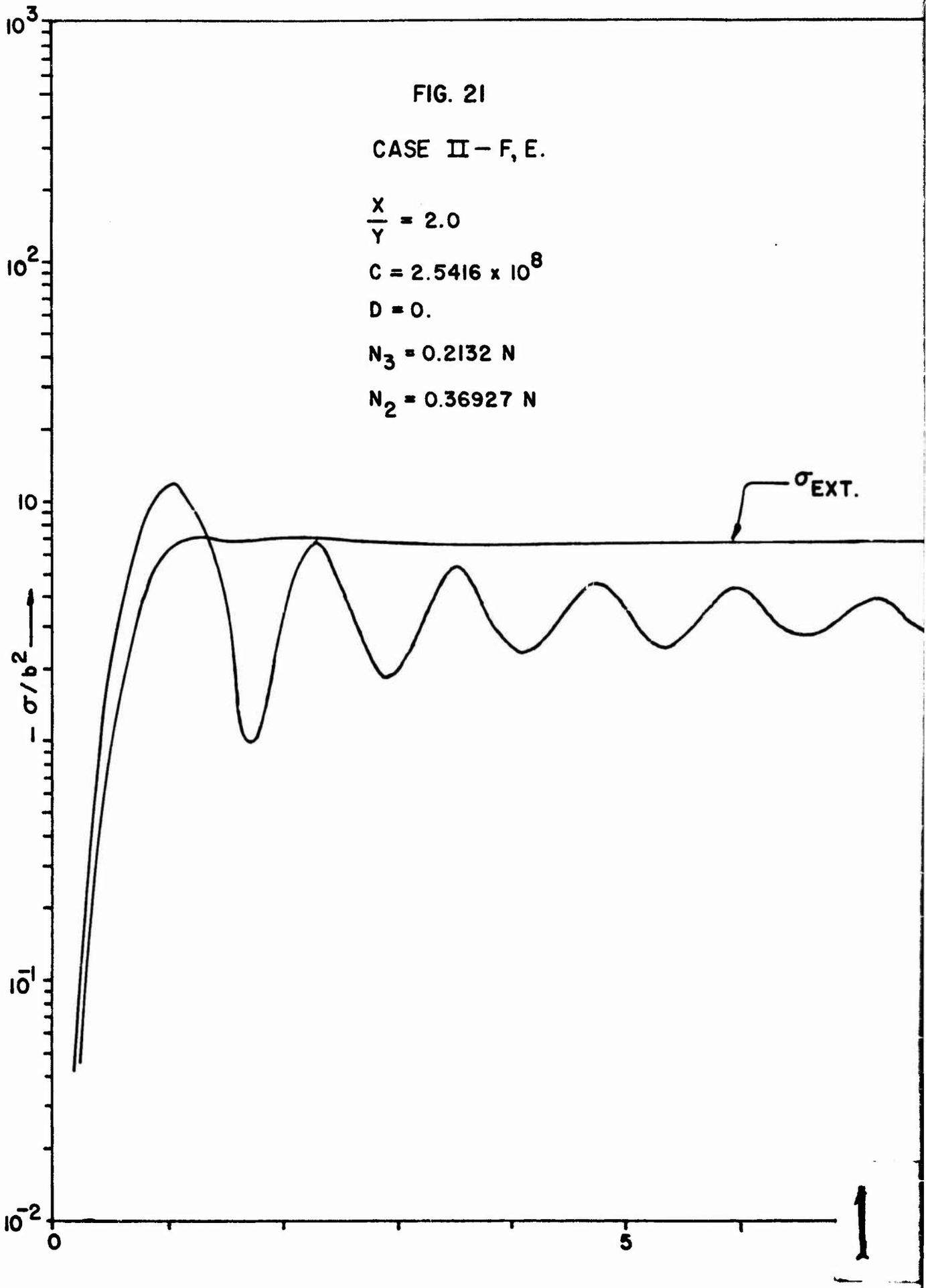
FIG. 21
CASE II – F, E.
X/Y = 2.0
C = 2.5416 x 10^8
D = 0.
N3 = 0.2132 N
N2 = 0.36927 N
σEXT.
10^3
10^2
10
10^-1
10^-2
- σ/b^2
0
5

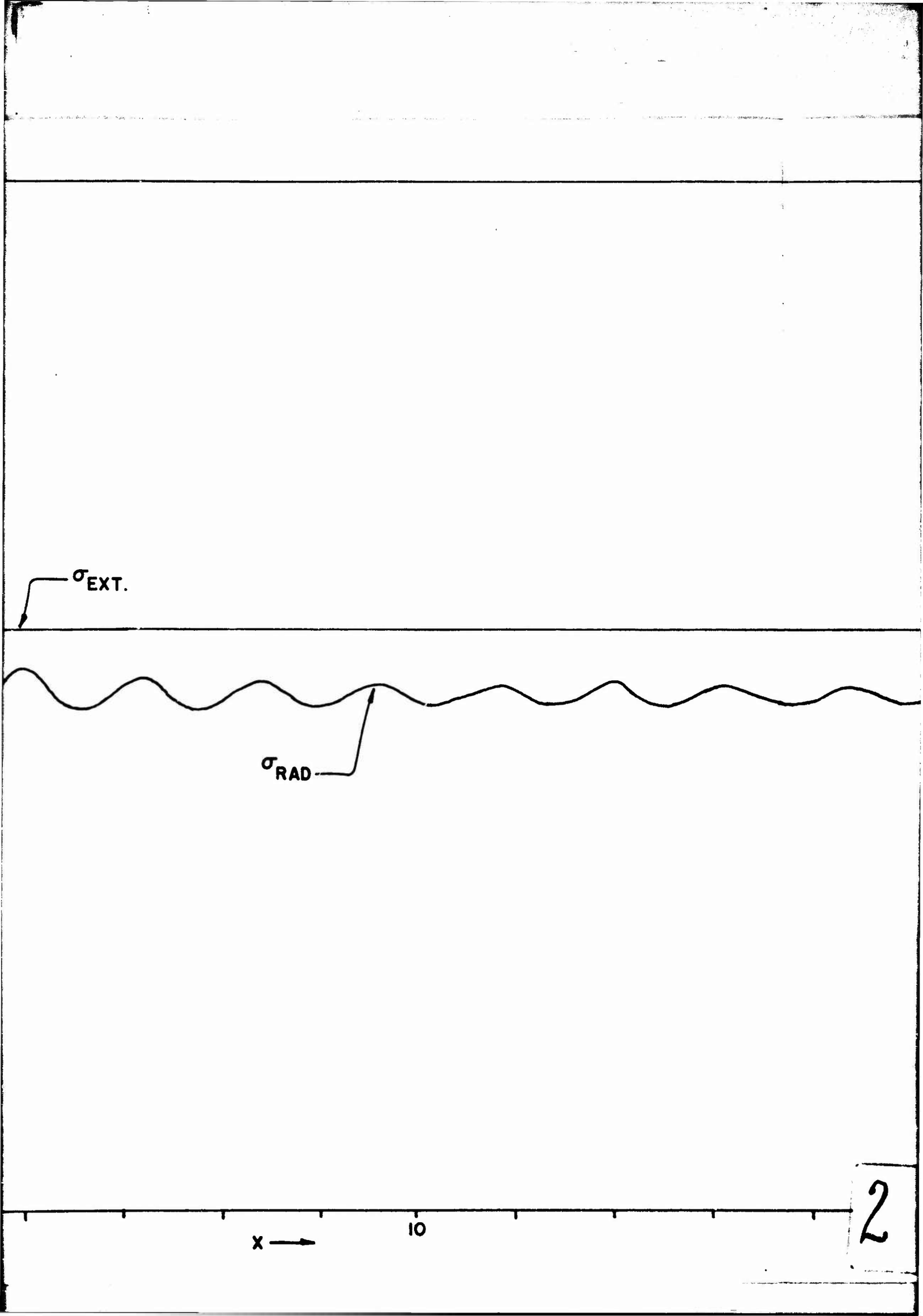
$\sigma_{EXT.}$
σ_{RAD}
10
X

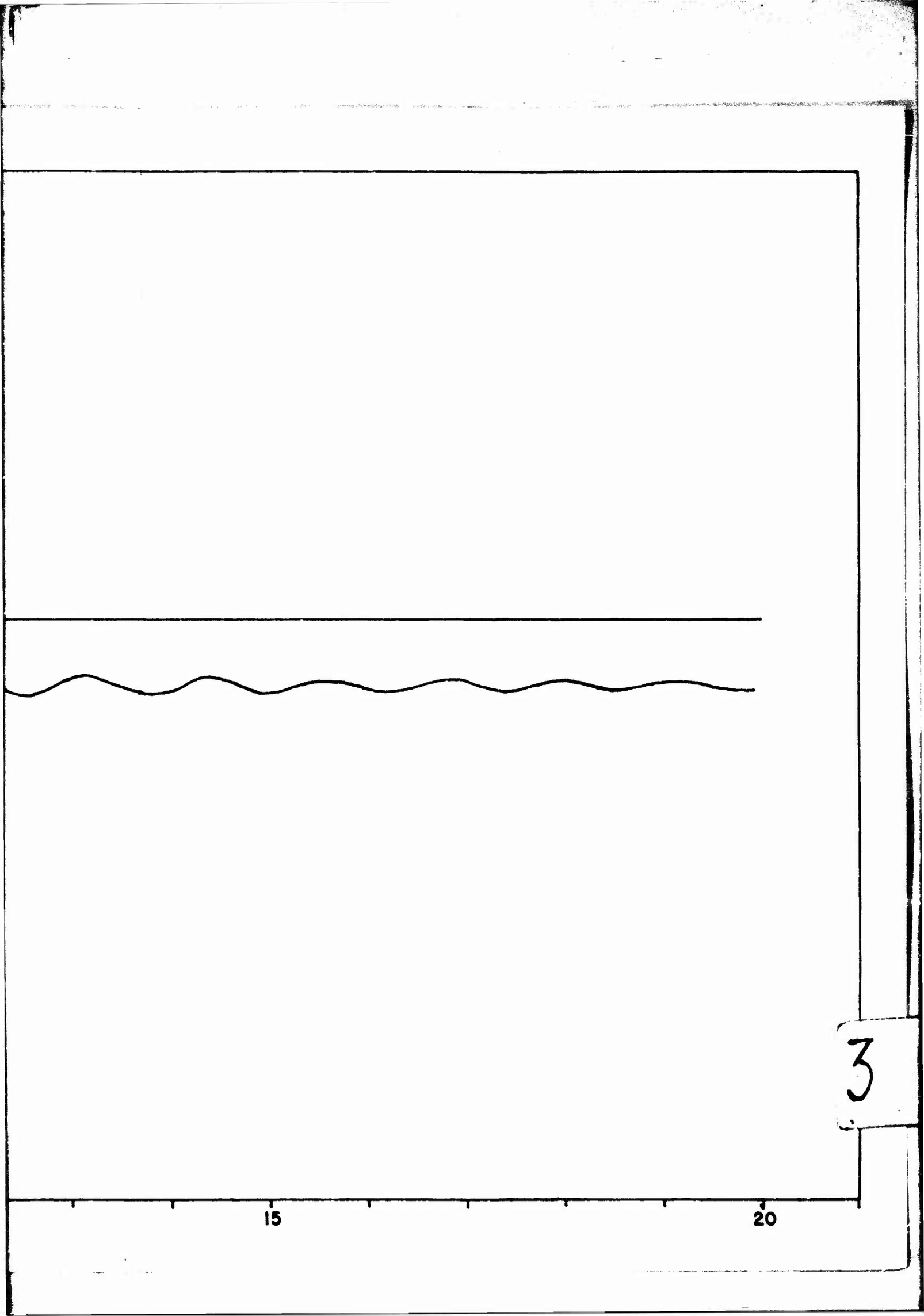
15
20

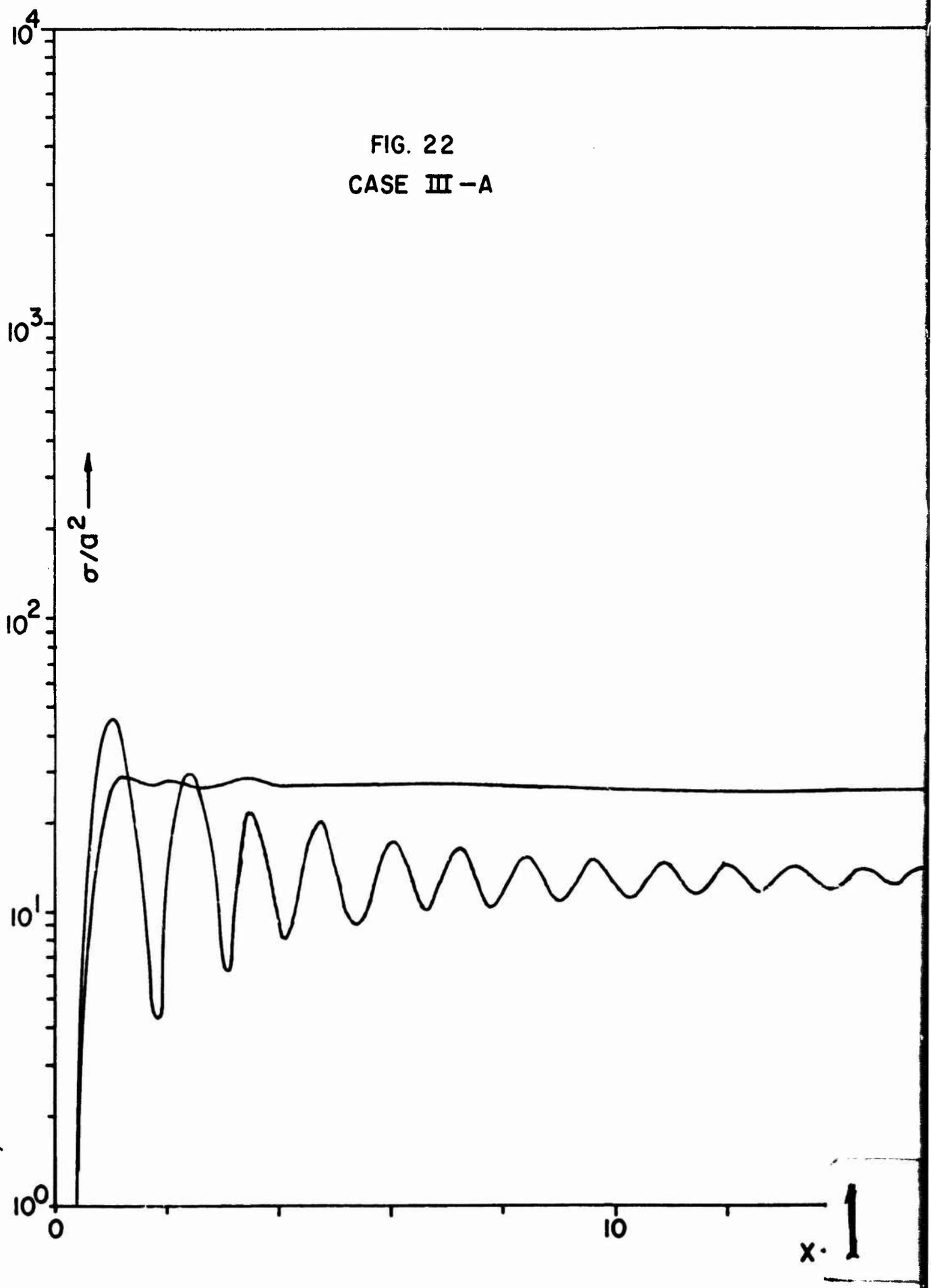
FIG. 22
CASE III – A
10^4
10^3
10^2
10^1
10^0
σ/a^2
0
10
x

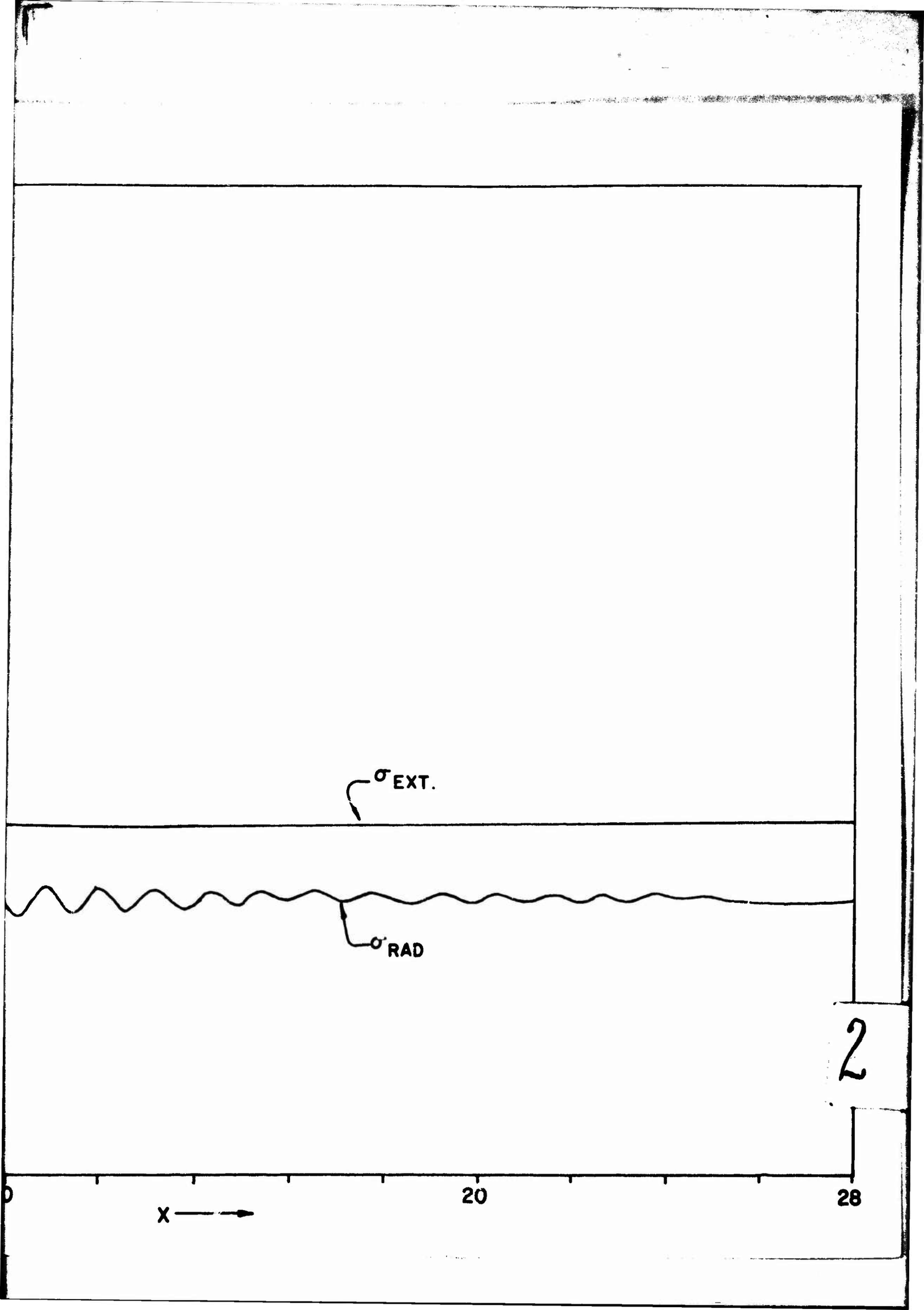

2

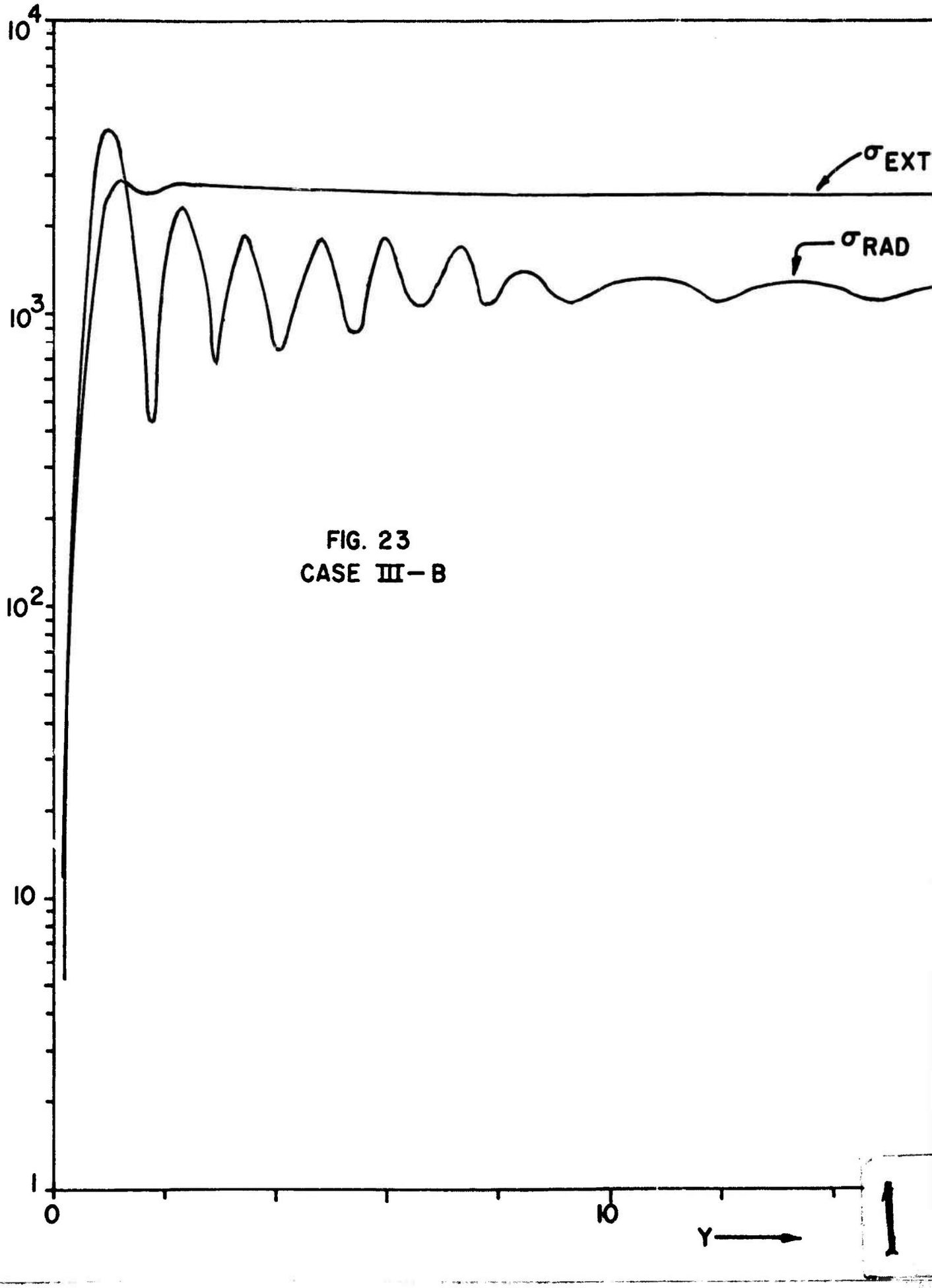

FIG. 23
CASE III – B

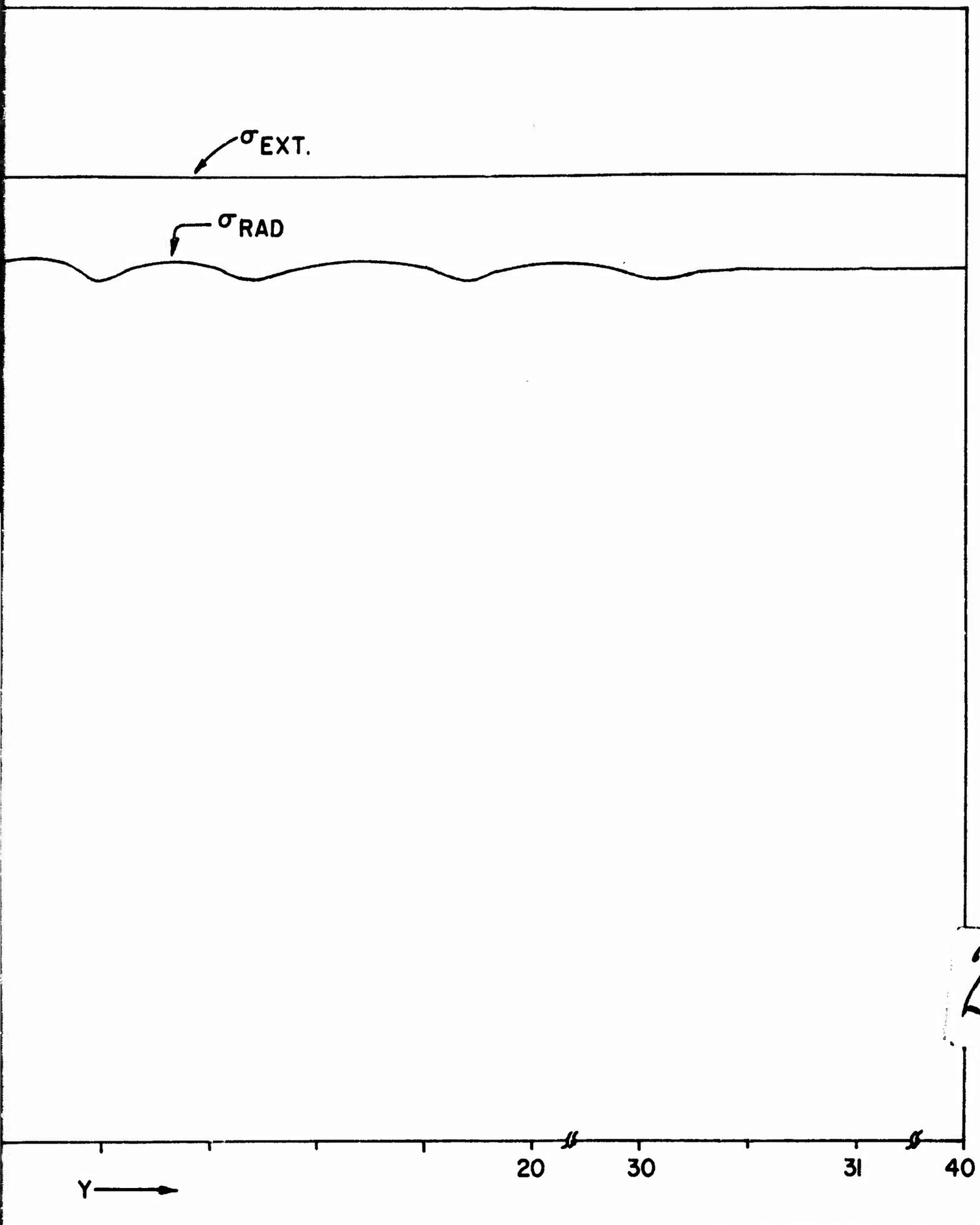

2

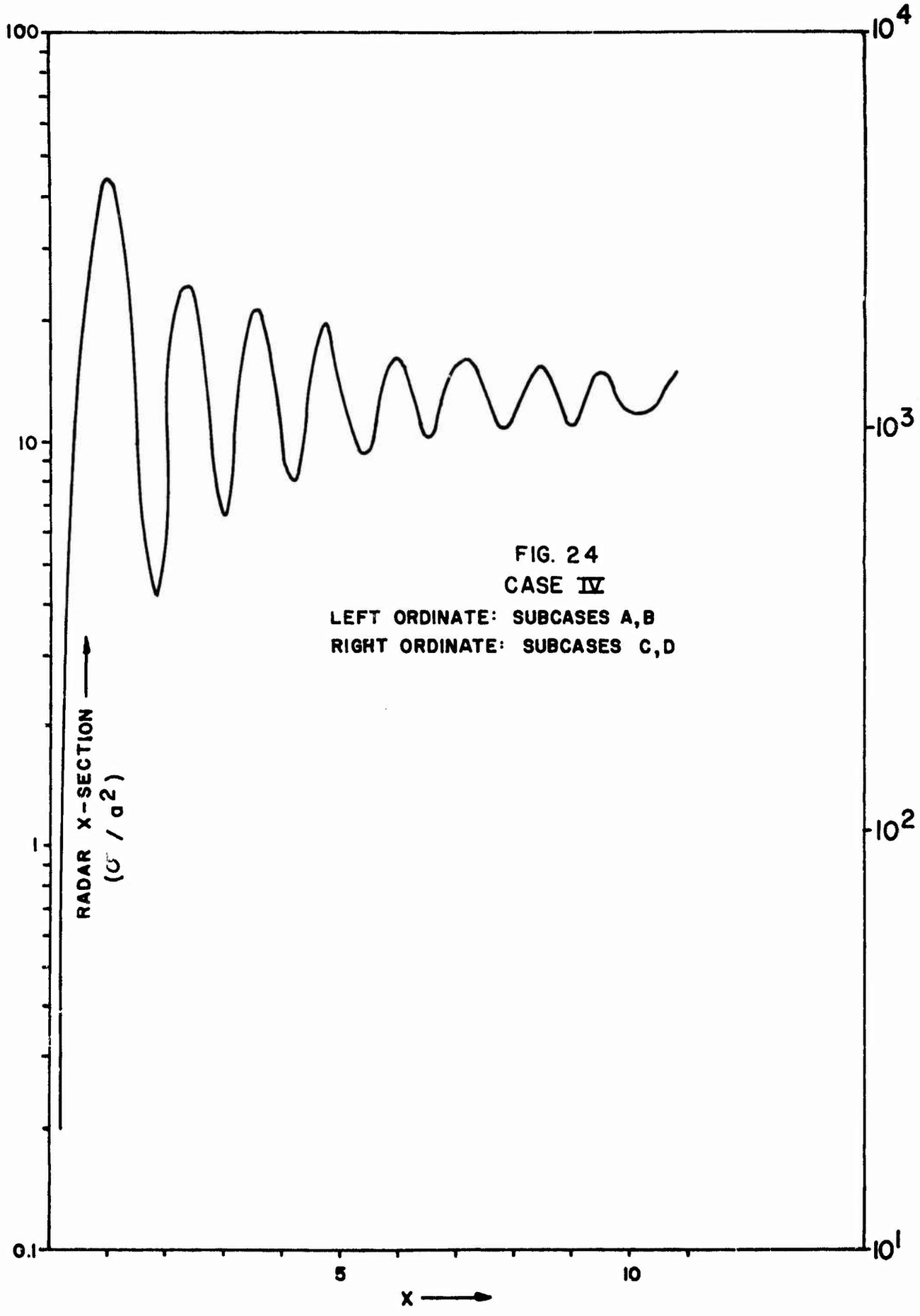

FIG. 24
CASE IV
LEFT ORDINATE: SUBCASES A, B
RIGHT ORDINATE: SUBCASES C, D

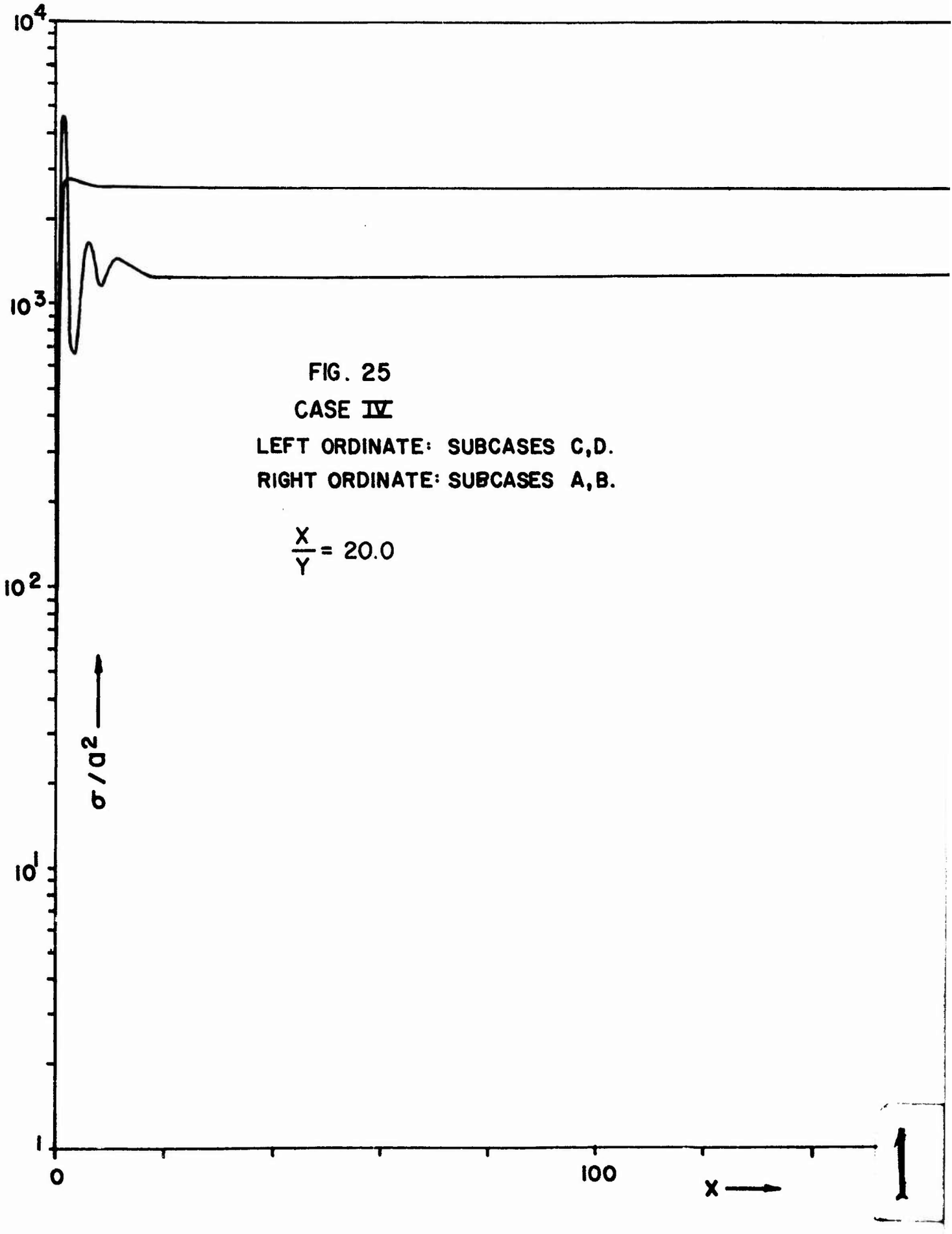

FIG. 25

CASE IV

LEFT ORDINATE: SUBCASES C,D.

RIGHT ORDINATE: SUBCASES A,B.

$\frac{X}{Y} = 20.0$

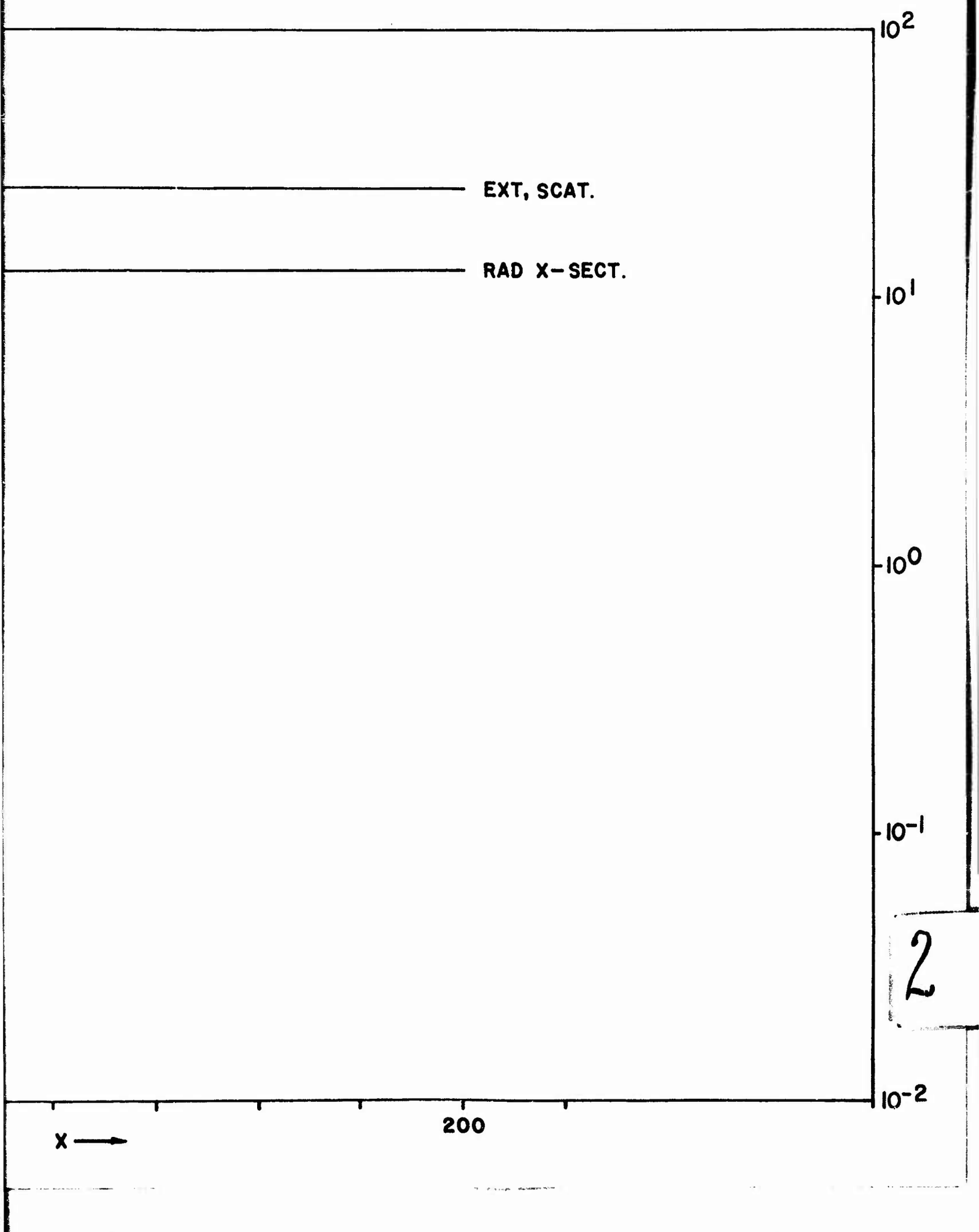

2

UNCLASSIFIED

Security Classification

DOCUMENT CONTROL DATA - R&D

(Security classification of title, body of abstract and indexing annotation must be entered when the overall report is classified)

1. ORIGINATING ACTIVITY (Corporate author) Astrophysics Research Corporation 10889 Wilshire Blvd., Suite 455 Los Angeles, California 90024	2a. REPORT SECURITY CLASSIFICATION Unclassified 2b GROUP None

3. REPORT TITLE

Radar Cross Sections of Inhomogeneous Plasma Spheres
Part II - Applications (U)

4. DESCRIPTIVE NOTES (Type of report and inclusive dates)

Scientific

5. AUTHOR(S) (Last name, first name, initial)

Erma, Victorr A.

6. REPORT DATE	7a. TOTAL NO. OF PAGES	7b. NO. OF REFS
15 February 1967		2

8a. CONTRACT OR GRANT NO.	9a. ORIGINATOR'S REPORT NUMBER(S)
Nonr 4527(00) b. PROJECT NO.	TR-018
c. d.	9b. OTHER REPORT NO(S) (Any other numbers that may be assigned this report)

10. AVAILABILITY/LIMITATION NOTICES

This document is subject to special export controls, and each transmittal to foreign governments or foreign nations may be made only with prior approval of the Office of Naval Research, Field Projects Brach, Washington, D. C. 20360

11. SUPPLEMENTARY NOTES	12. SPONSORING MILITARY ACTIVITY
None	Office of Naval Research Code 418 Washington 25, D. C.

13 ABSTRACT

The present work has been concerned with the numerical evaluation of the exact analytical expressions obtained in Part I[1] for the scattering from radially inhomogeneous plasma spheres of different electron density profiles. Several computer programs were developed for this purpose. These programs are capable of handling a wide range of values of the physical parameters, and are of potential value to many research programs concerned with the scattering of electromagnetic waves from plasma spheres. Numerical data were calculated for a number of representative cases characteristic of high-altitude plasma clouds. Configurations of both radially increasing and decreasing electron density profiles were evaluated. The plasma spheres considered generally had radii of 100-200 m, with electron densities of the order $10^{18} m^{-3}$. Radar cross sections for these spheres were computed for the entire range of frequencies. For purposes of greater physical understanding of the numerical results obtained, analytical approximations to the exact expressions were developed for the Rayleigh region. Finally, the existence of the anomalous backscatter region in the cross section profile of overdense plasmas was confirmed.

DD FORM 1 JAN 64 1473

UNCLASSIFIED

Security Classification

UNCLASSIFIED

Security Classification

14 KEY WORDS	LINK A		LINK B		LINK C	
	ROLE	WT	ROLE	WT	ROLE	WT
Radar Cross-Sections Scattering Cross-Sections Electromagnetic Scattering Plasma Clouds Inhomogeneous Plasma Spheres Electromagnetic Waves Diffraction						

INSTRUCTIONS

1. ORIGINATING ACTIVITY: Enter the name and address of the contractor, subcontractor, grantee, Department of Defense activity or other organization *(corporate author)* issuing the report.

2e. REPORT SECURITY CLASSIFICATION: Enter the overall security classification of the report. Indicate whether "Restricted Data" is included. Marking is to be in accordance with appropriate security regulations.

2b. GROUP: Automatic downgrading is specified in DoD Directive 5200.10 and Armed Forces Industrial Manual. Enter the group number. Also, when applicable, show that optional markings have been used for Group 3 and Group 4 as authorized.

3. REPORT TITLE: Enter the complete report title in all capital letters. Titles in all cases should be unclassified. If a meaningful title cannot be selected without classification, show title classification in all capitals in parenthesis immediately following the title.

4. DESCRIPTIVE NOTES: If appropriate, enter the type of report, e.g., interim, progress, summary, annual, or final. Give the inclusive dates when a specific reporting period is covered.

5. AUTHOR(S): Enter the name(s) of author(s) as shown on or in the report. Enter last name, first name, middle initial. If military, show rank and branch of service. The name of the principal author is an absolute minimum requirement.

6. REPORT DATE: Enter the date of the report as day, month, year; or month, year. If more than one date appears on the report, use date of publication.

7a. TOTAL NUMBER OF PAGES: The total page count should follow normal pagination procedures, i.e., enter the number of pages containing information.

7b. NUMBER OF REFERENCES: Enter the total number of references cited in the report.

8a. CONTRACT OR GRANT NUMBER: If appropriate, enter the applicable number of the contract or grant under which the report was written.

8b, 8c, & 8d. PROJECT NUMBER: Enter the appropriate military department identification, such as project number, subproject number, system numbers, task number, etc.

9a. ORIGINATOR'S REPORT NUMBER(S): Enter the official report number by which the document will be identified and controlled by the originating activity. This number must be unique to this report.

9b. OTHER REPORT NUMBER(S): If the report has been assigned any other report numbers *(either by the originator or by the sponsor)*, also enter this number(s).

10. AVAILABILITY/LIMITATION NOTICES: Enter any limitations on further dissemination of the report, other than those imposed by security classification, using standard statements such as:

(1) "Qualified requesters may obtain copies of this report from DDC."

(2) "Foreign announcement and dissemination of this report by DDC is not authorized."

(3) "U. S. Government agencies may obtain copies of this report directly from DDC. Other qualified DDC users shall request through

_____."

(4) "U. S. military agencies may obtain copies of this report directly from DDC. Other qualified users shall request through

_____."

(5) "All distribution of this report is controlled. Qualified DDC users shall request through

_____."

If the report has been furnished to the Office of Technical Services, Department of Commerce, for sale to the public, indicate this fact and enter the price, if known.

11. SUPPLEMENTARY NOTES: Use for additional explanatory notes.

12. SPONSORING MILITARY ACTIVITY: Enter the name of the departmental project office or laboratory sponsoring *(paying for)* the research and development. Include address.

13. ABSTRACT: Enter an abstract giving a brief and factual summary of the document indicative of the report, even though it may also appear elsewhere in the body of the technical report. If additional space is required, a continuation sheet shall be attached.

It is highly desirable that the abstract of classified reports be unclassified. Each paragraph of the abstract shall end with an indication of the military security classification of the information in the paragraph, represented as *(TS)*, *(S)*, *(C)*, or *(U)*.

There is no limitation on the length of the abstract. However, the suggested length is from 150 to 225 words.

14. KEY WORDS: Key words are technically meaningful terms or short phrases that characterize a report and may be used as index entries for cataloging the report. Key words must be selected so that no security classification is required. Identifiers, such as equipment model designation, trade name, military project code name, geographic location, may be used as key words but will be followed by an indication of technical context. The assignment of links, rules, and weights is optional.

UNCLASSIFIED

Security Classification